Progress towards the realization of quantum computer architectures in silicon and diamond

Thomas Schenkel

Lawrence Berkeley National Laboratory

Contact: T_Schenkel@LBL.gov, 510-486-6674

CS-191, guest lecture, 70 Evans, UC Berkeley, Nov. 17, 2009

Progress towards the realization of quantum computer architectures in silicon and diamond

1. Introduction
2. Spin readout transistors
3. Single Atom Doping
4. First results from Spins in Diamond
5. Outlook

Evolution of computational power

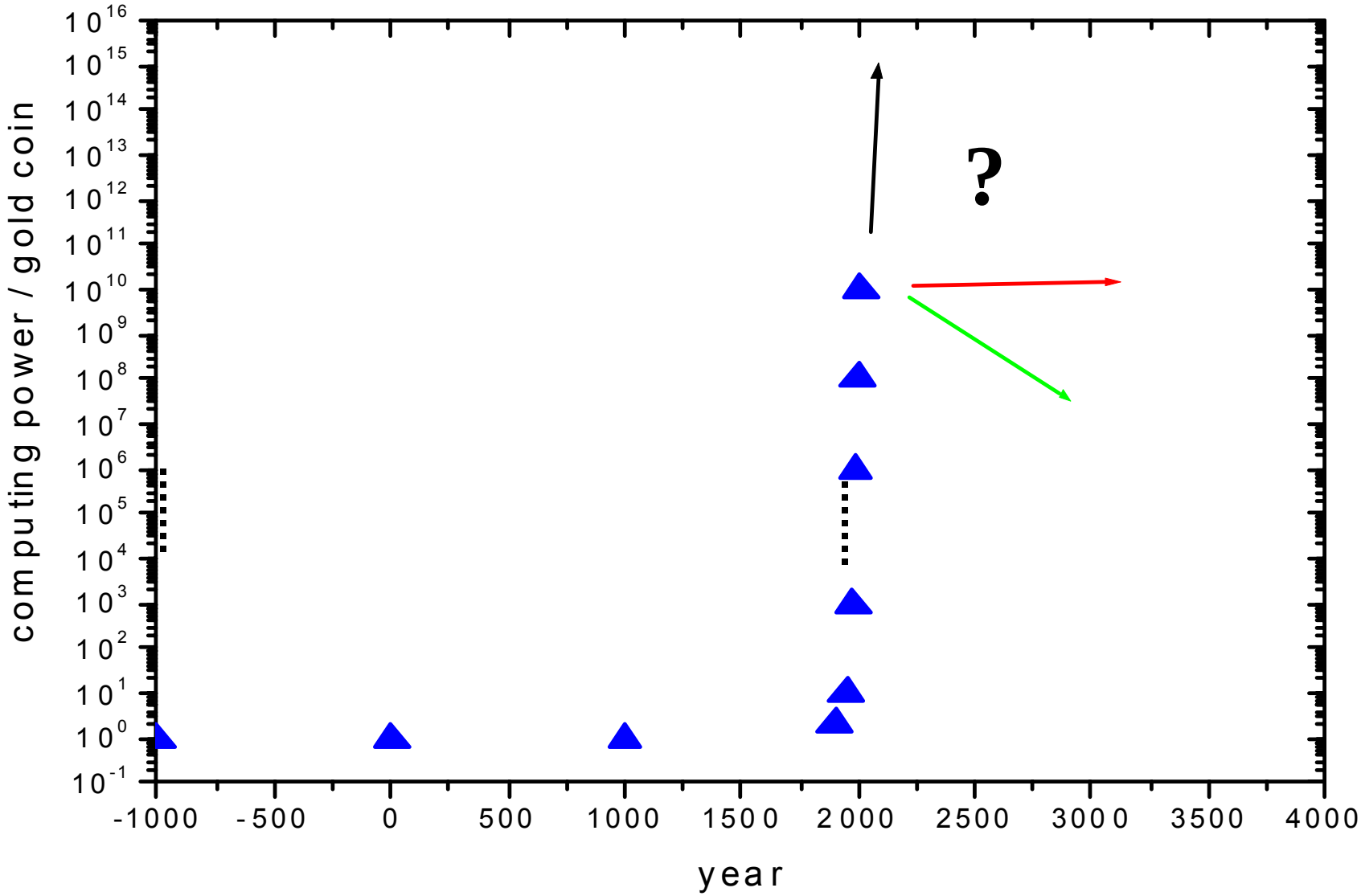

Wave-particle duality of C_{60} molecules

Wave **superposition of "which path" states in double slits leads to interference**

Particle **interaction of molecules with environment destroys interference, (decoherence, and "classical" behavior)**

→ Quantum info processing requires the coherent superposition of N qubits !

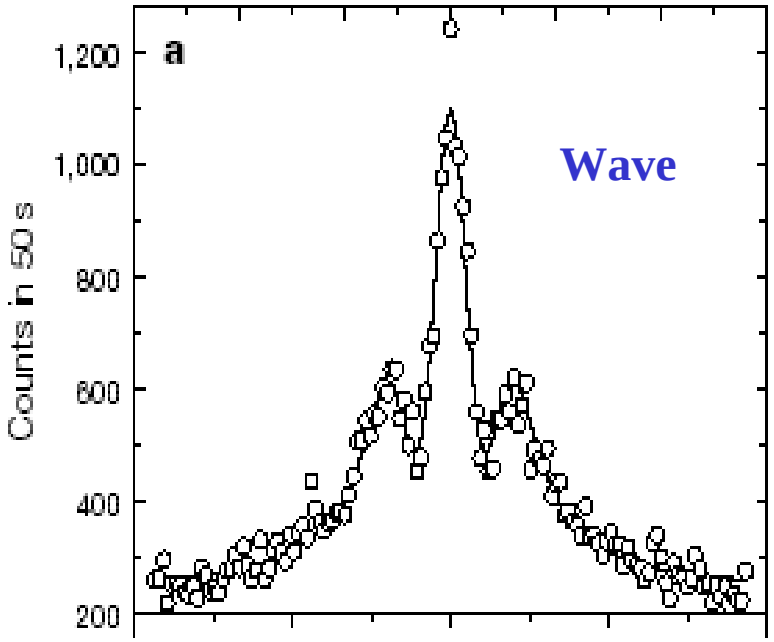

Markus Arndt, Olaf Nairz, Julian Vos-Andreae, Claudia Keller, Gerbrand van der Zouw & Anton Zeilinger

Institut für Experimentalphysik, Universität Wien, Boltzmanngasse 5, A-1090 Wien, Austria

NATURE | VOL 401 | 14 OCTOBER 1999 |

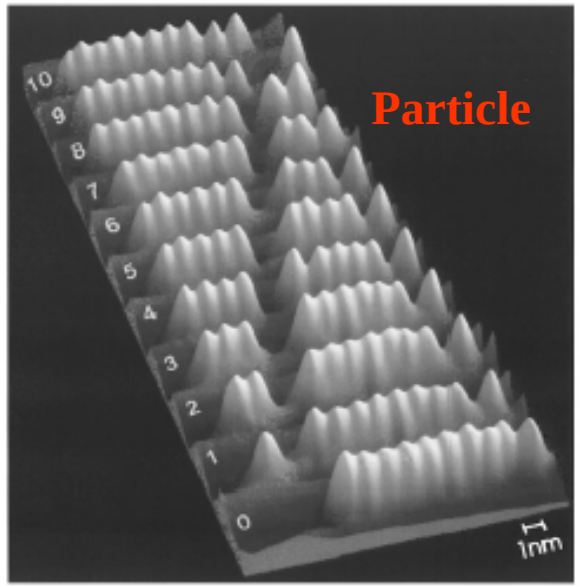

Room-temperature repositioning of individual C_{60} molecules at Cu steps: Operation of a molecular counting device

M. T. Cuberes,[a)] R. R. Schlittler, and J. K. Gimzewski
IBM Research Division, Zurich Research Laboratory, 8803 Rüschlikon, Switzerland

Appl. Phys. Lett. **69** (20), 11 November 1996

The Quest for Quantum Computing

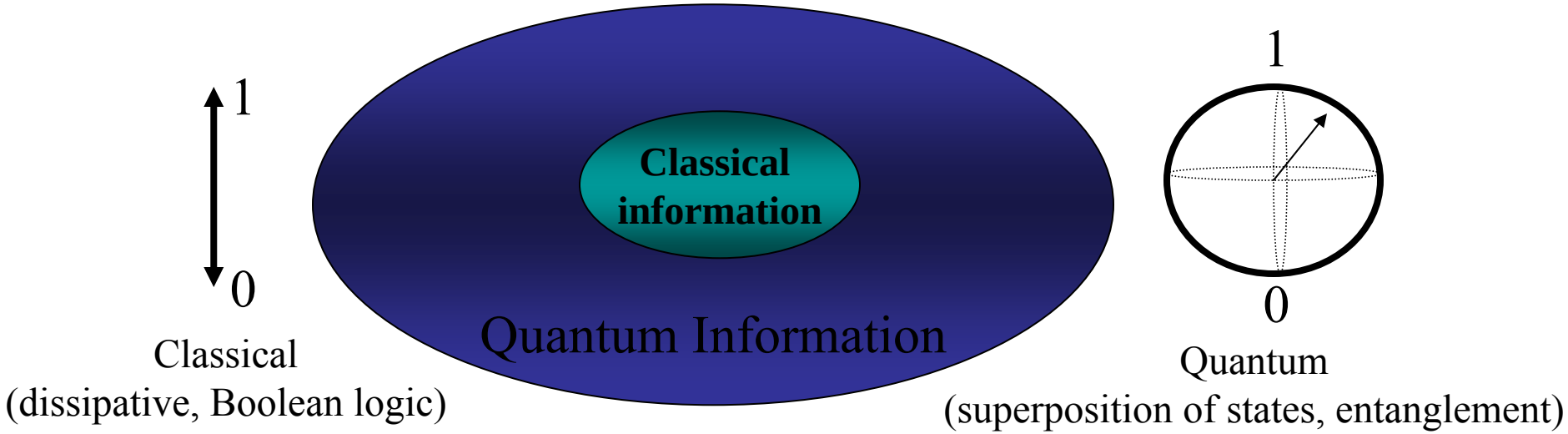

Two paths towards quantum computing:

- take a quantum system and see if one can use it to compute ("soup paradigm", e. g. NMR)
- or, take a computer architecture and see if it can function coherently ("device paradigm")

also:

- quest for post-CMOS logic motivates search for new ways to encode information beyond classical charge based computing (e. g. spin)

Why in solids?

Scalability -

Classical transistor scaling and quantum computer development converge

"Moore's Law" (Gordon Moore, Intel)
exponentially more, cheaper, faster and smaller transistors

more

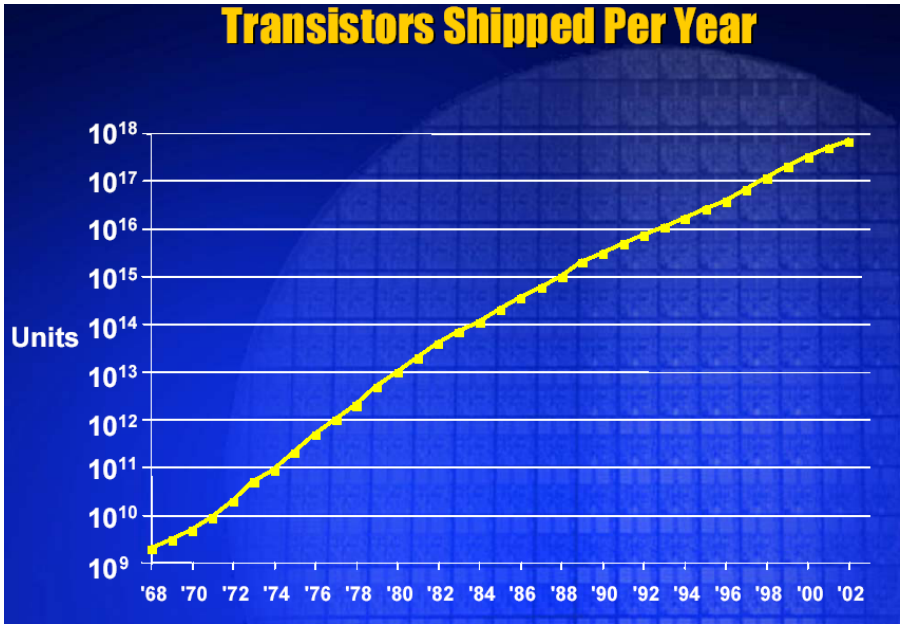

cheaper

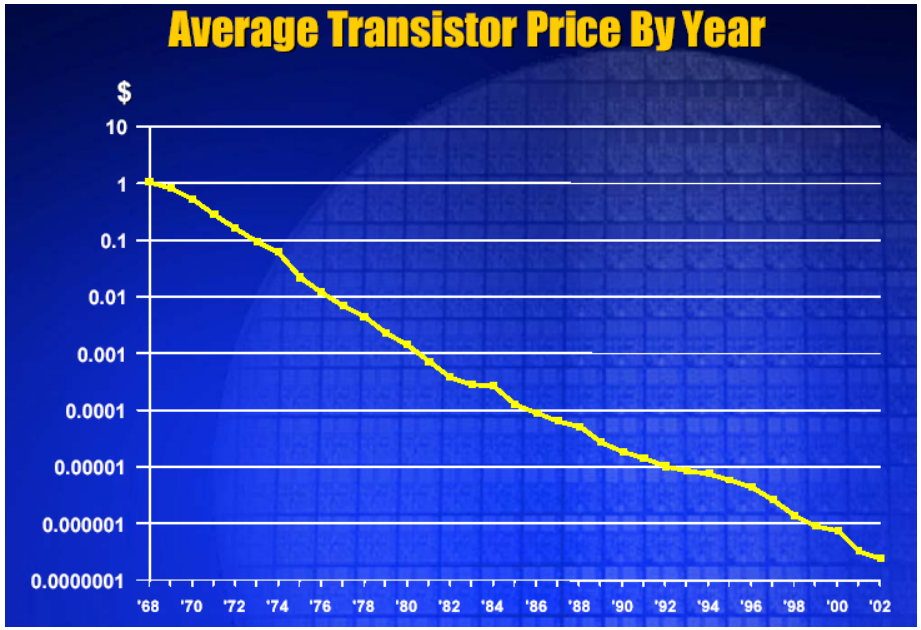

More transistors made each year then raindrops fall on California

Moore's Law of exponential speedup of silicon transistors: *faster*

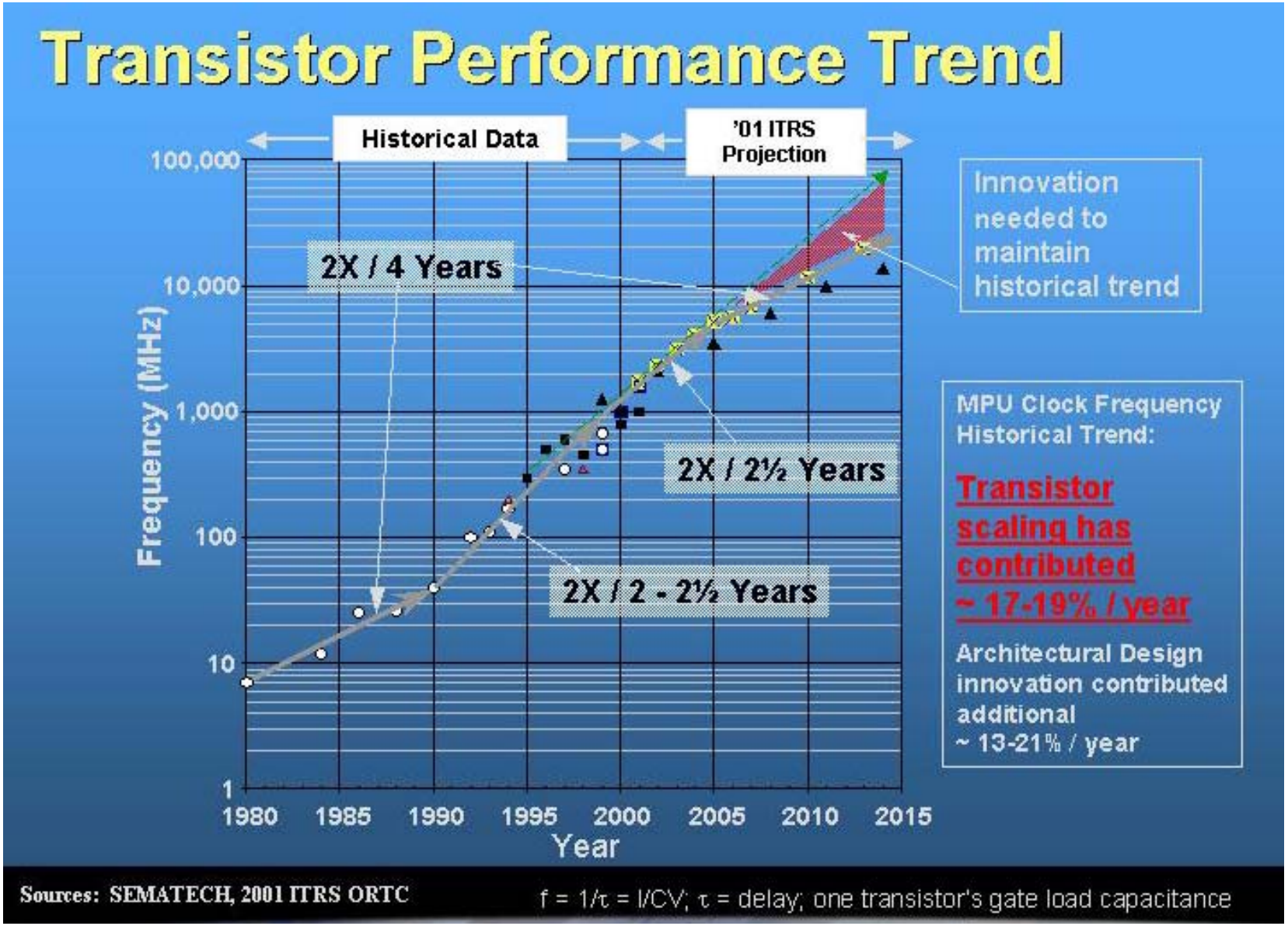

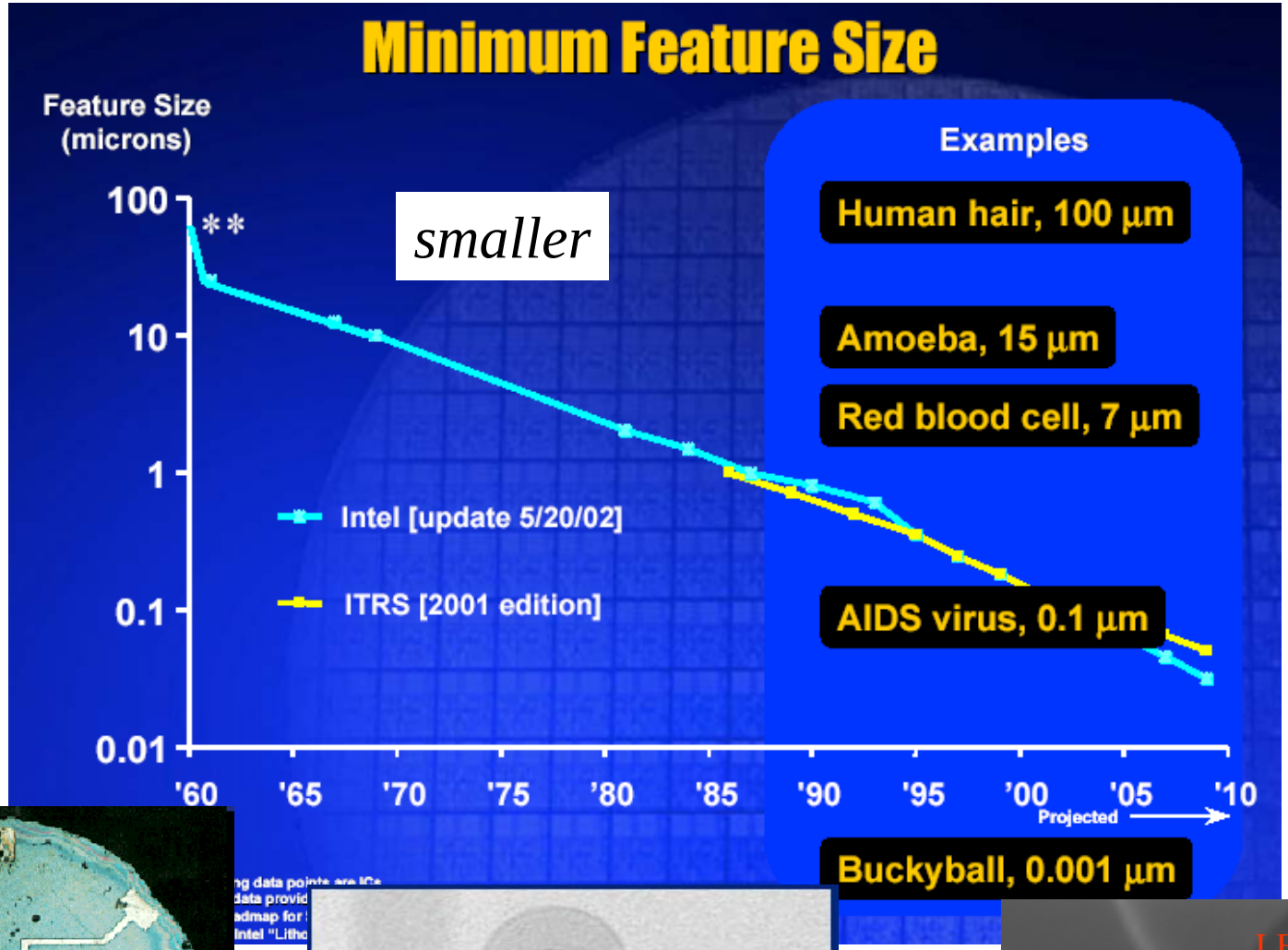
Minimum Feature Size
Feature Size (microns)
100
10
1
0.1
0.01
**
smaller
Intel [update 5/20/02]
ITRS [2001 edition]
'60
'65
'70
'75
'80
'85
'90
'95
'00
'05
'10
Projected
Examples
Human hair, 100 µm
Amoeba, 15 µm
Red blood cell, 7 µm
AIDS virus, 0.1 µm
Buckyball, 0.001 µm

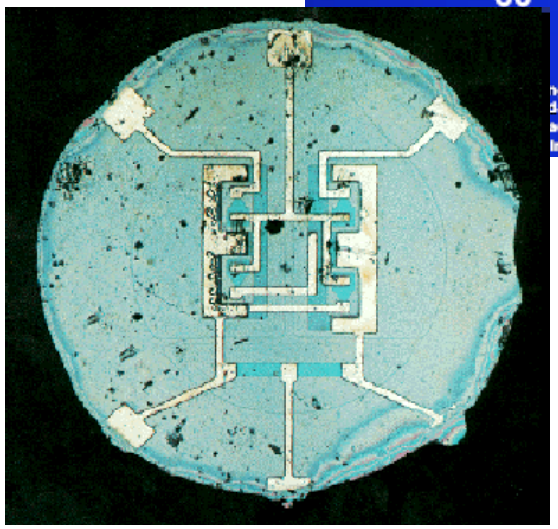

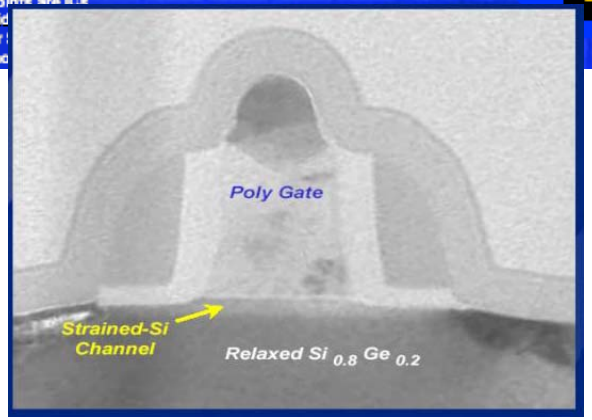
Poly Gate
Strained-Si Channel
Relaxed Si 0.8 Ge 0.2

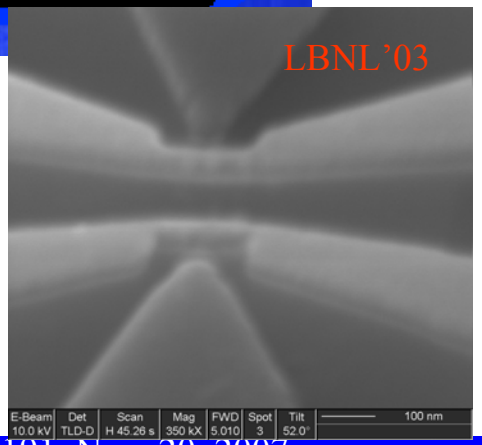
LBNL'03
100 nm

Donor electron spin qubits in silicon

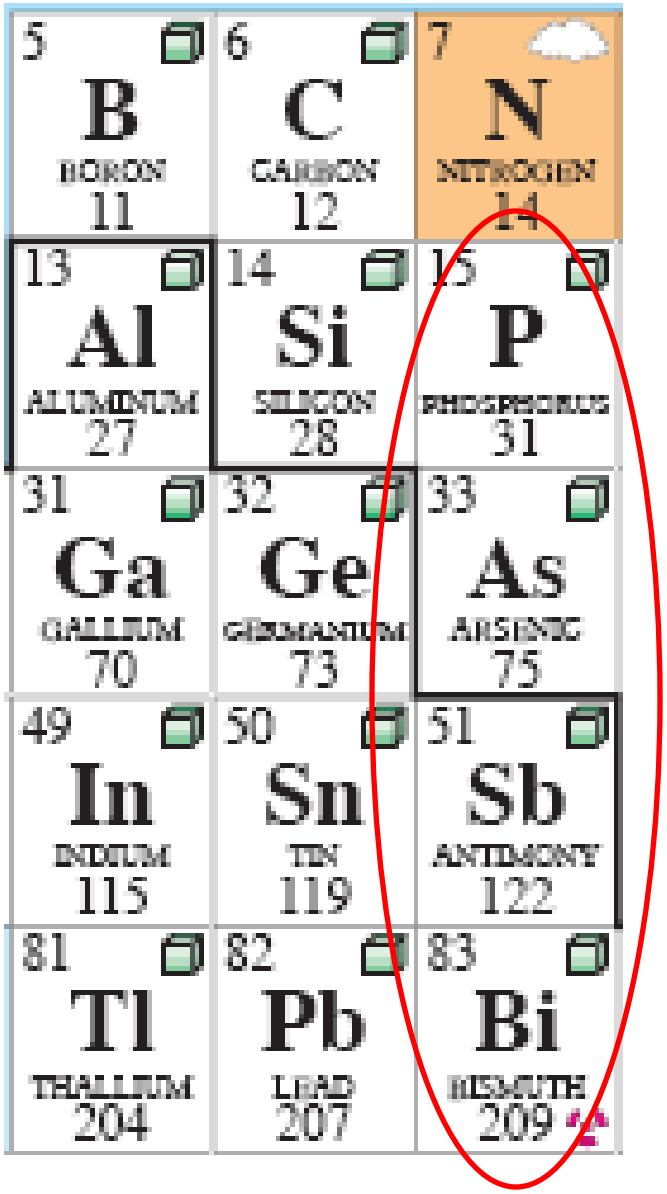

^{31}P ("natural quantum dot")

Si: [Ne].3s^2.3p^2

P: [Ne].3s^2.3p^3

- 3p^3 binding energy: 45 meV
- 100% abundant isotope with I=1/2
- ^{28}Si matrix can be prepared with I=0

Qubits:
electron and nuclear spins of donor atoms in silicon

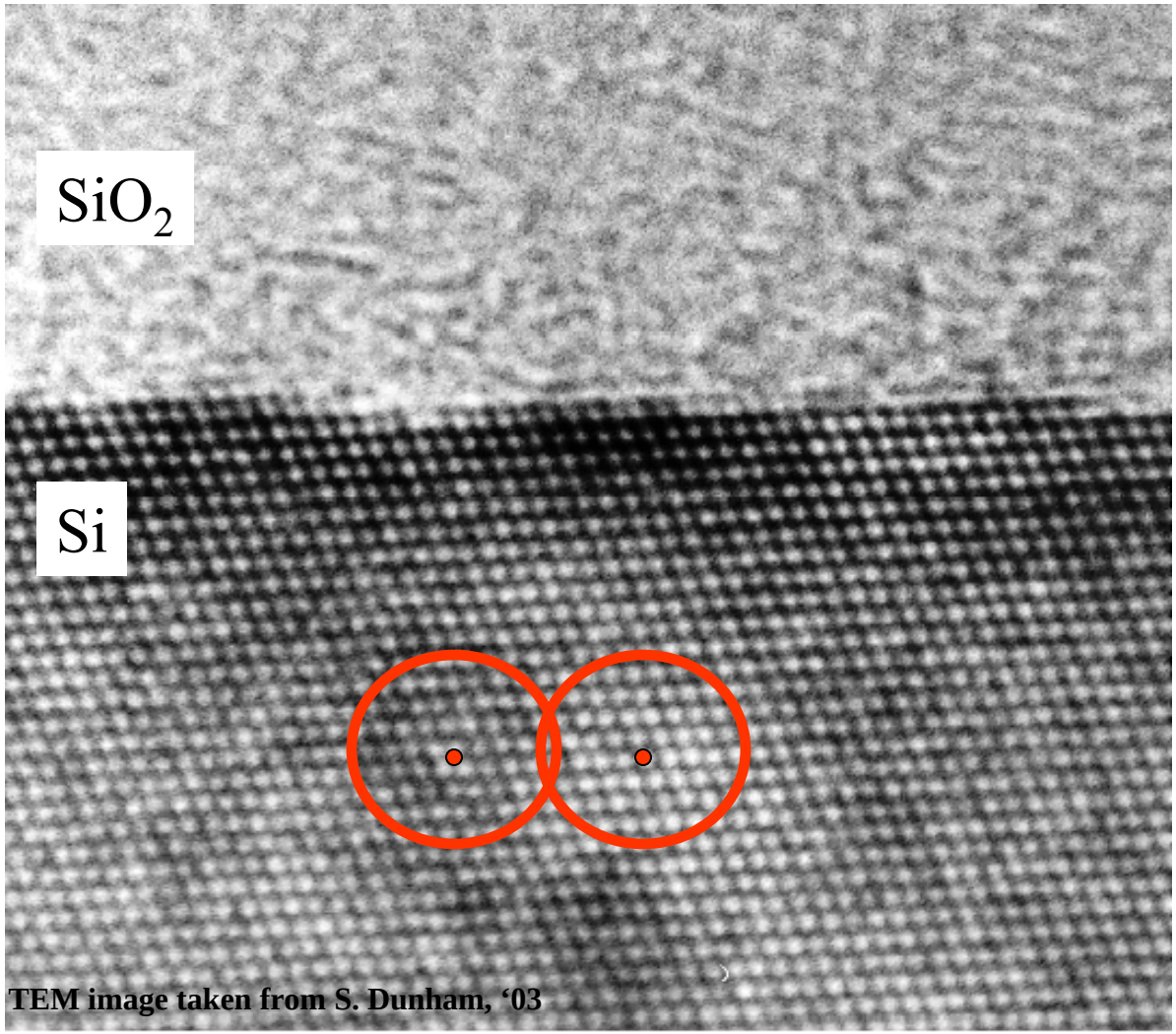

TEM image taken from S. Dunham, '03

• Long decoherence times
-nuclear spin: >1 s
-electron spin: tens of ms

• Bohr radius of bound,
3p electron of ^{31}P in Si: ~2 nm

$$a_0 = \varepsilon_{Si} \frac{m_0}{m_{eff}} \; \varepsilon_0 \frac{h^2}{\pi \, m_0 q^2} =$$

$$= \varepsilon_{Si} \frac{m_0}{m_{eff}} \; 0.53 \, \mathring{A}$$

$$(\varepsilon_{Si} = 12)$$

Criteria for physical implementation of a quantum computer (DiVincenzo)

1. Well defined extendible qubit array – stable memory
2. Initialization in the "000…" state
3. Long decoherence time (>10^4 operation time, to allow for error correction)
4. Universal set of gate operations (not, cnot)
5. Read-out: Single-quantum measurements (projective measurement)
6. Efficient quantum communication (form, transmit and convert "flying qubits")

donor spins in silicon: "natural quantum dots"

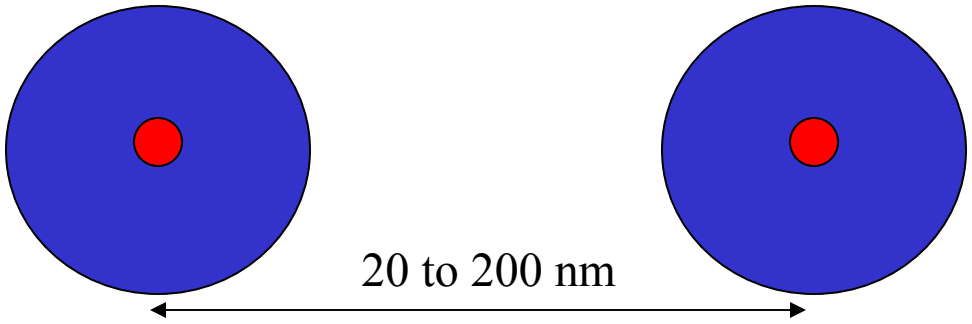

The Quest for Quantum Computing

- several quantum computer architectures with single atom based qubits
  - electron and nuclear spins of donors in silicon (Kane ’98)
  - electron and nuclear spins of NV^- centers in diamond

→ need for device integration of single atoms

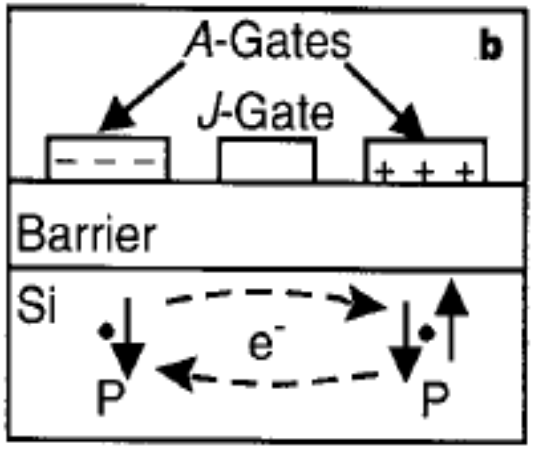

Kane, Nature, 1998

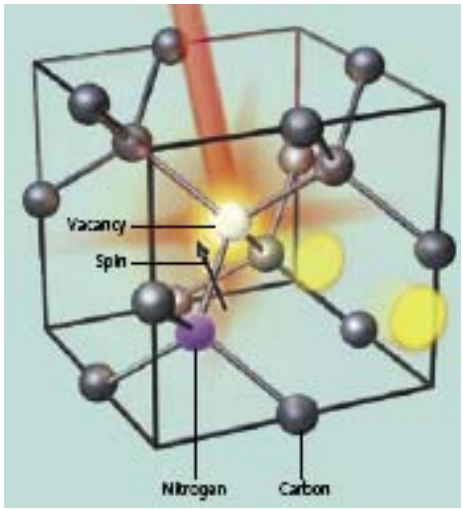

Awschalom et al., Sci. Amer. ‘07

Why quantum computation with spins in silicon and diamond ?

0. Why Quantum Computation ?

- Information storage capacity of N qubits ~2^N
- Quantum algorithms promise speedups through parallel, unitary qubit evolution
- General paradigm of quantum information theory

1. Why in solids ?

- Promise of scalability to large N (>10^6)

2. Why in Silicon ?

- Device requirements converting with trends in classical silicon transistor technology
- Long coherence times for electron and nuclear spins of donor atoms at 5 K
  - **Why not in Silicon ?**
  - No single spin readout (yet), no clear path to long range coupling (donor – dot – cavity ?)

3. Why in diamond ?

- Long coherence times of N and NV^- spins (~ 1 ms) at room temperature
- Optical access, control of single spin centers (NV^-), coupling (NV-N, NV-^{13}C) demonstrated
  - **Why not in diamond ?**
  - Limited materials availability (~mm pieces), poor process control (no SPER)

Towards -*coherent*- single atom electronics

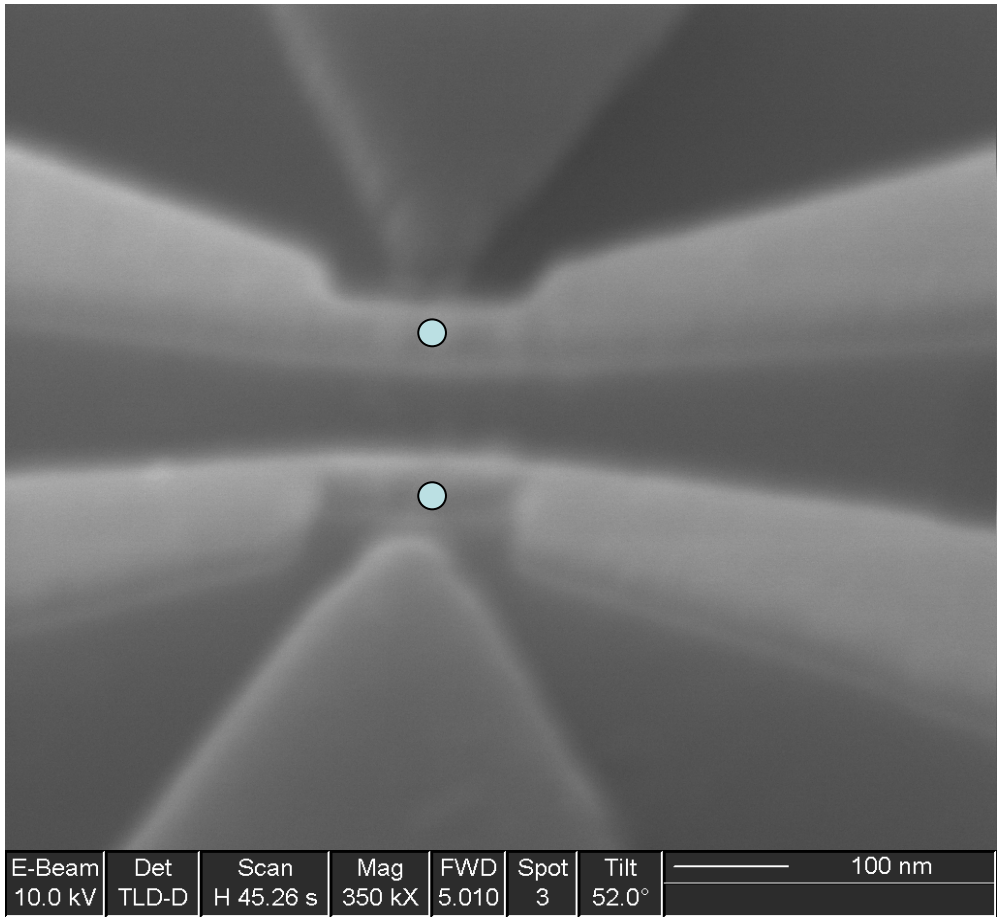

"Atoms are large"
Characteristic length scale in silicon devices: Bohr radius

$$2 \times a_0 = 2 \times \varepsilon_{Si} \frac{m_0}{m_{eff}} \quad 0.53 \overset{o}{A} \approx 3-4 \ \ nm$$

$$(\varepsilon_{Si} = 11.8, \ m_{eff} \approx 0.2 \ \ m_0)$$

- "easy" lithographic access to 10-20 nm scale
- transport properties sensitive to presence of single dopant atoms

→ understanding single dopant effects can benefit CMOS scaling

- **can we control, couple and readout states of single atom qubits coherently ?**

→ **test of quantum computing architectures**

•Si-SETs: S. J. Park, et al., J. Vac. Sci. Technol. 22, 3115 (2004)

Berkeley Lab
UC Berkeley
Princeton

Path to quantum logic demonstrations with donor electron spin qubits in silicon

1. **Develop devices for single spin readout**
   - Spin dependent transport in transistors

2. **Develop a technique for qubit array formation**
   - Single ion implantation with Scanning Probe alignment

3. **Process and materials studies for T_2 optimization**
   - Spin dynamics in pre-device structures

4. **Demonstration of quantum logic**
   - Formulate logic protocol by mapping of physical interactions to qubit gates

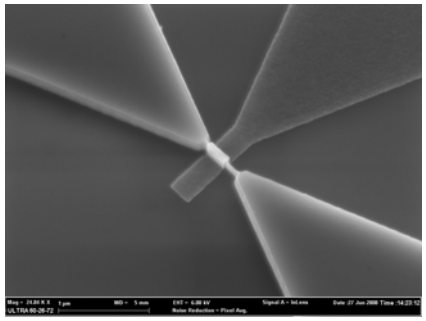

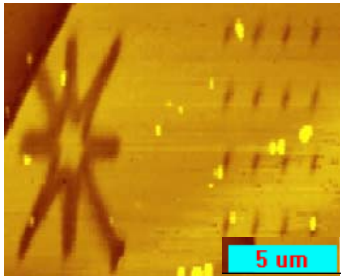

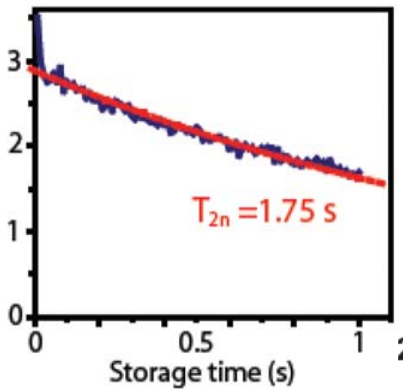

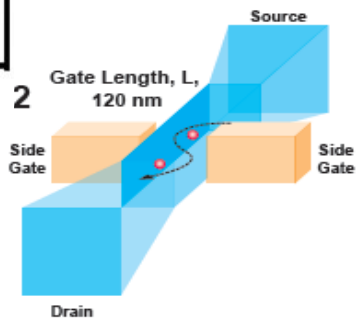

• theory – fabrication – measurement QCCM collaboration between LBNL (T. Schenkel – PI), UC Berkeley (J. Bokor, B. Whaley), and Princeton University (S. Lyon, A. Tyryshkin)

1. Introduction

2. Spin readout transistors

3. Single Atom Doping

4. Outlook

Spin Readout Mechanism

- Single nuclear spin-state detection for donor qubits by spin-dependent neutral impurity scattering[1]:

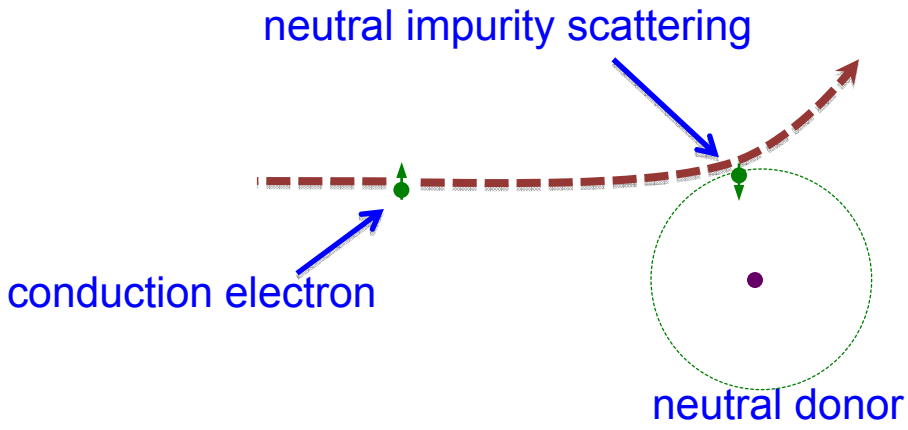

  - Measurements for devices with ~10^{4}-10^{6} donors[2]
  - Understand scaling behavior & signal enhancement
- Non-equilibrium spin polarization detection in silicon

[1]Sarovar et al., PRB, 78, 245302 (2008)

[2]Lo et al., APL, 91, 242106 (2007)

Towards readout of a single donor electron (and nuclear) spin state in a transistor

- Detection of single donor electron spin state through formation of D^- states, which have to be singlet states, thus enabling spin to charge conversion (Kane '98)
- Projective and quantum non demolition measurements through encoding of quantum information in nuclear spin states (**M. Sarovar et al, arXiv:0711.2343**)

→ spin dependent neutral impurity scattering between conduction electrons and donor atoms in field effect transistor channels is a mechanism that can enable single spin state readout

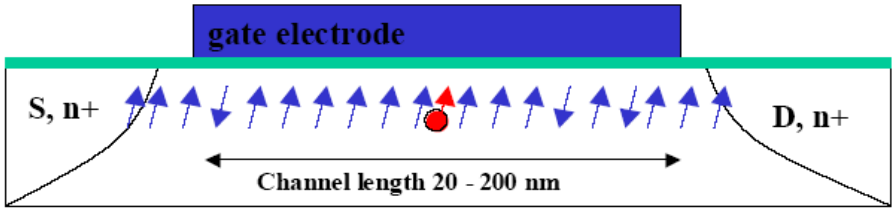

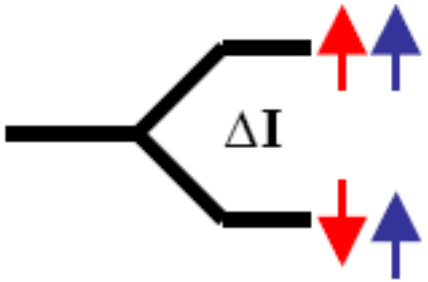

$$\frac{\Delta I}{I} \sim P_d^0 P_{ce}^0 \left(\frac{\Sigma_S - \Sigma_T}{\Sigma_S + 3\Sigma_T} \right) \frac{1/\tau_n}{1/\tau_{tot}}$$

- Early work in bulk doped devices by Ghosh and Silsbee, PRB 46, 12508 (1992)

PHYSICAL REVIEW B VOLUME 43, NUMBER 2 15 JANUARY 1991-I

Elastic scattering of electrons by neutral donor impurities in silicon

K. C. Kwong, J. Callaway, and N. Y. Du*
Department of Physics and Astronomy, Louisiana State University, Baton Rouge, Louisiana 70803-4001

R. A. LaViolette
Rockwell International Science Center, 3370 Miraloma Avenue, Anaheim, California 92803-3105
(Received 4 September 1990)

We consider the elastic scattering of low-energy electrons by neutral donor impurities in silicon, taking account of the actual anisotropic many-valley conduction band. Necessary modifications of the standard formulas of elastic-scattering theory that result from band anisotropy are derived. S matrices are determined by the solution of a set of coupled differential equations in which the static Coulomb potential and approximate representations of exchange and polarization interactions appear. The scattering is strongly anisotropic and spin dependent, even at very low energies.

The spin dependence of the cross sections will probably not be of much importance in most applications. One will be concerned with the average over spin states ($\frac{1}{4}$ singlet + $\frac{3}{4}$ triplet). Some results for this are shown in

A cross section related to transport properties is

$$\sigma_t = \frac{1}{4\pi}\int d\Omega_i \int d\Omega_f (1-\cos\theta_{if})\frac{d\sigma}{d\Omega_f}\ , \qquad (25)$$

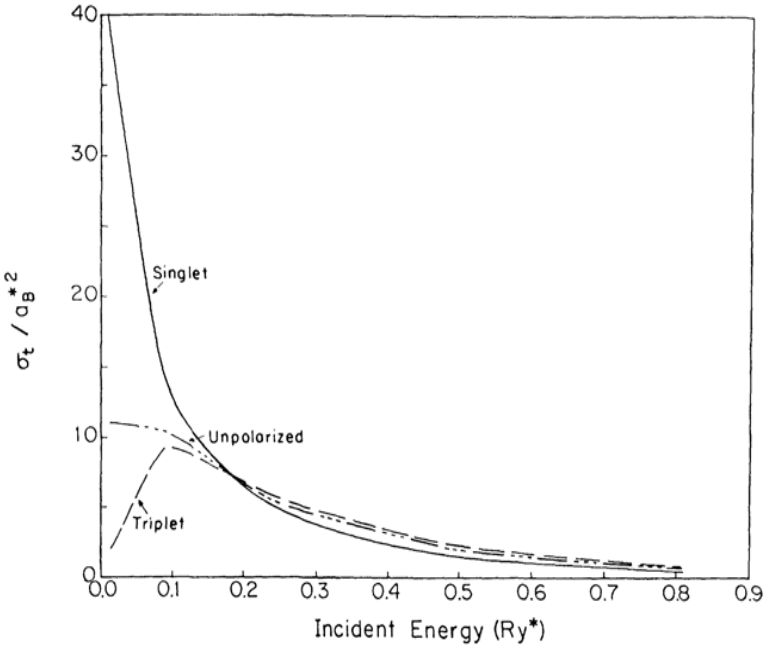

FIG. 5. Average transport cross section σ_T [Eq. (25)] as a function of incident energy. Singlet, triplet, and unpolarized results are shown.

Detection of Spin-dependent Scattering with EDMR

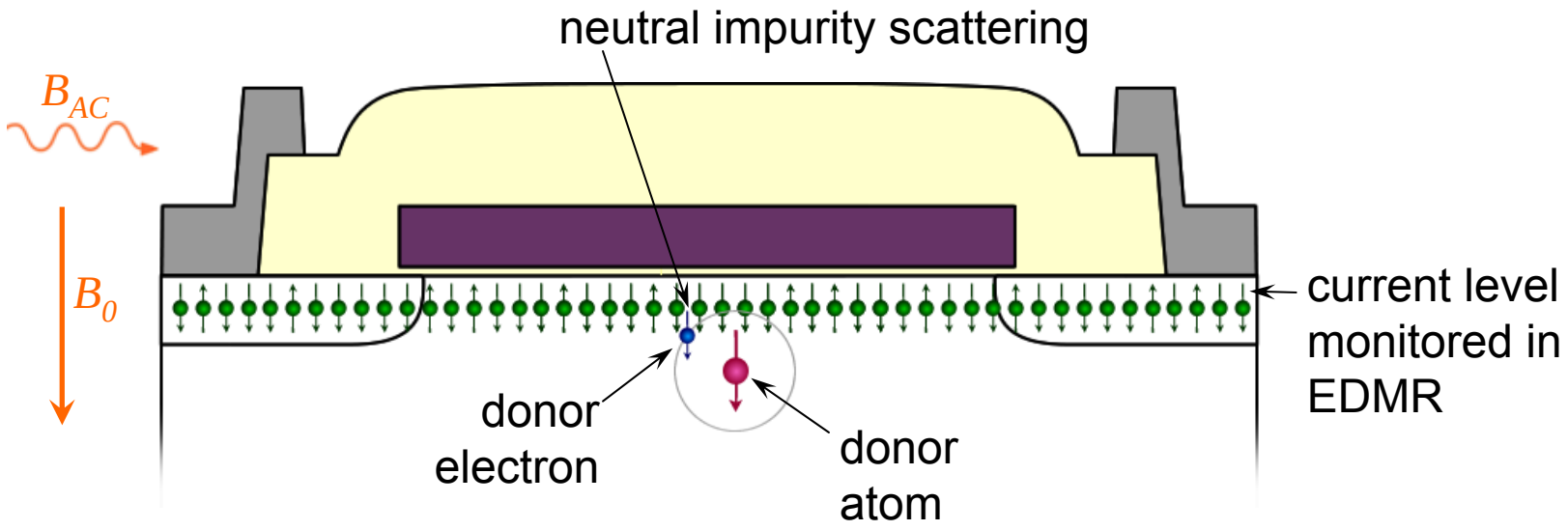

Off-resonance:

- Partial electron spin polarization due to Zeeman splitting from DC B-field
- More triplet scattering than in unpolarized spin population case

On-resonance (donor electrons/conduction electrons):

- Polarization of donor electrons/conduction electrons altered
- change in effective channel resistance due to increase in singlet scattering

Electrical Detection of Electron Spin Resonance

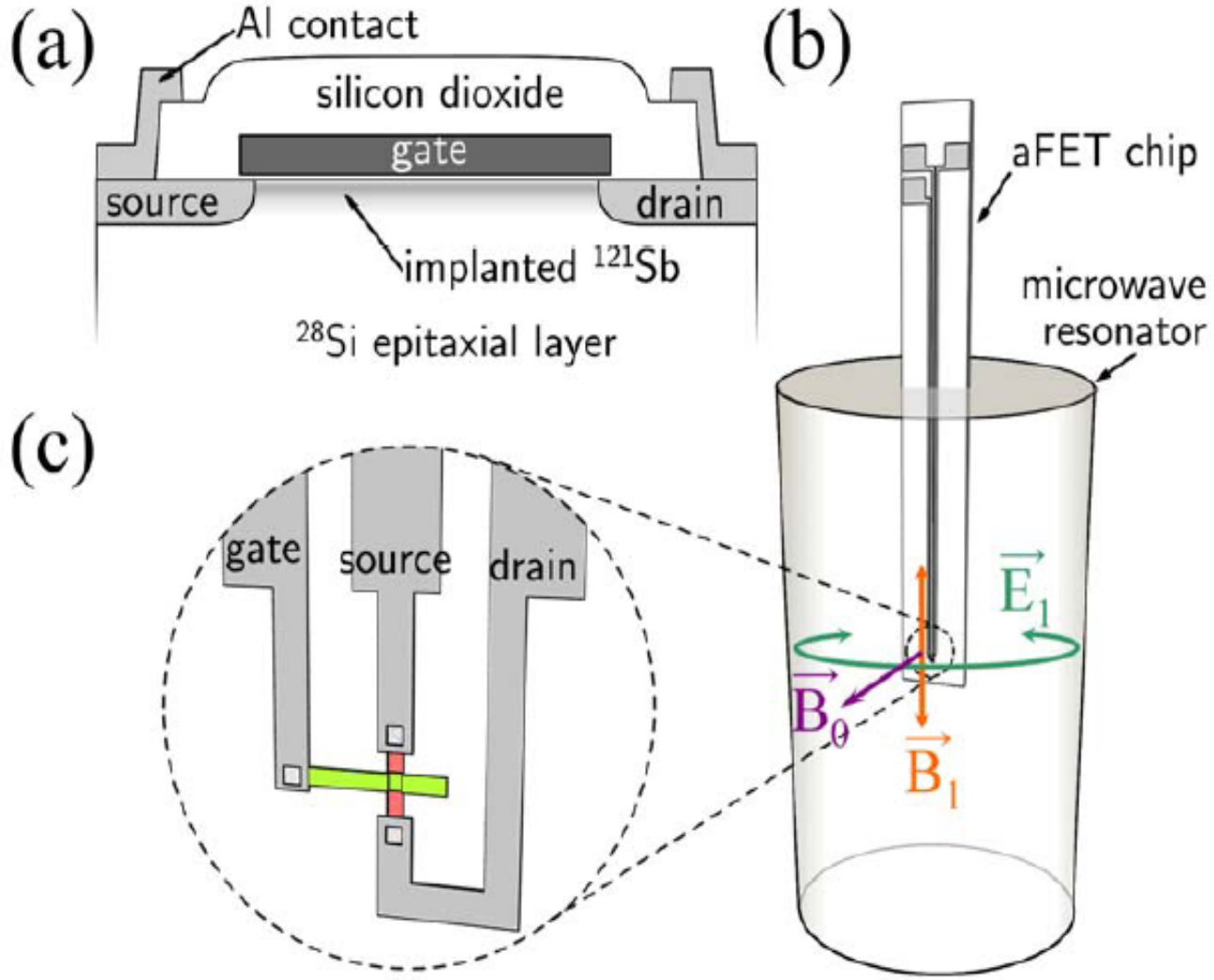

a) Schematic cross-section of an aFET. (b) Device placement and field orientations in the ESR microwave resonator. (c) Magnified view of an aFET chip.

- Cheuk C. Lo, et al., Appl. Phys.. Lett. 91, 242106 (2007)

EDMR Setup at Princeton (group of Steve Lyon)

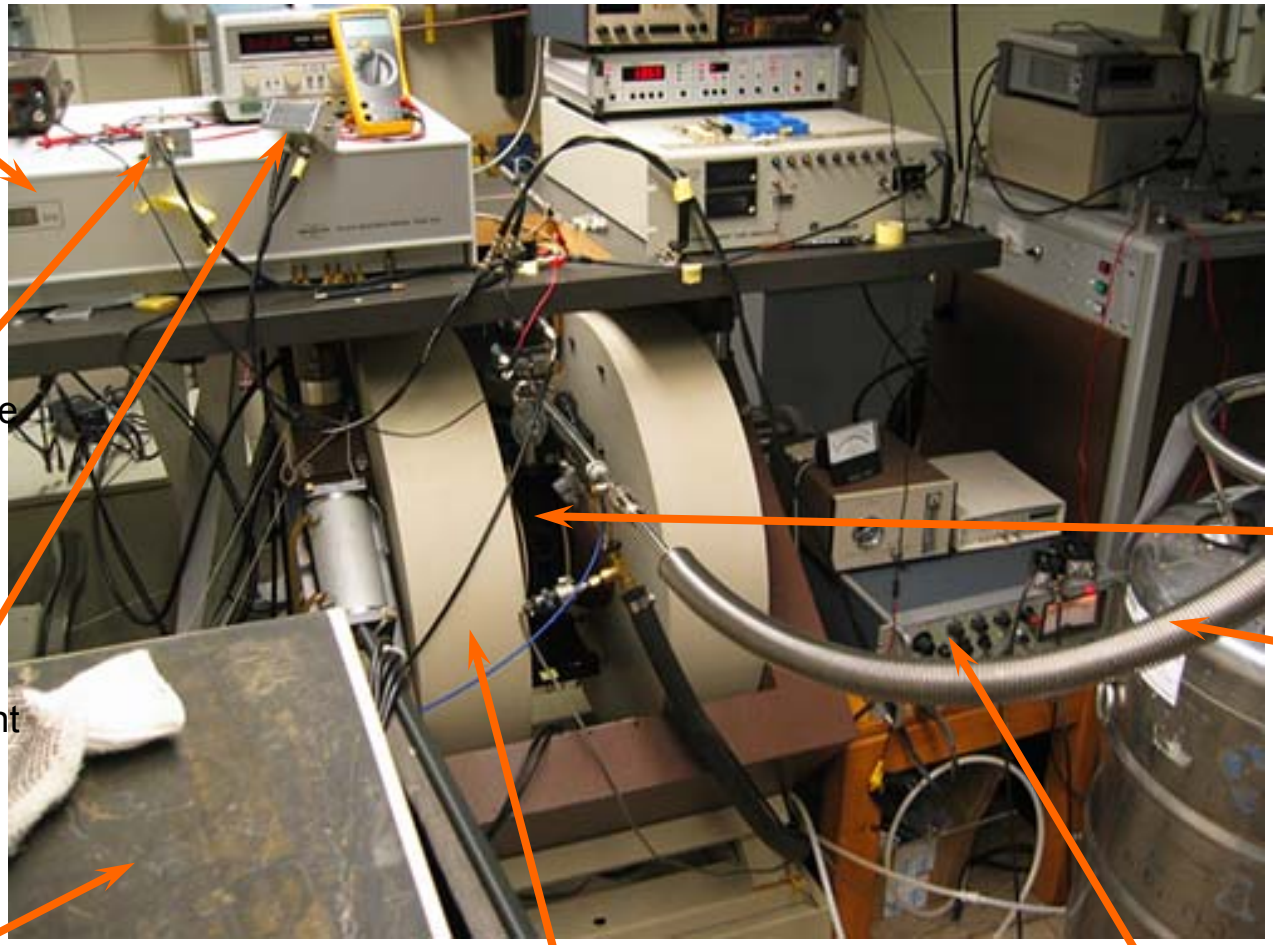

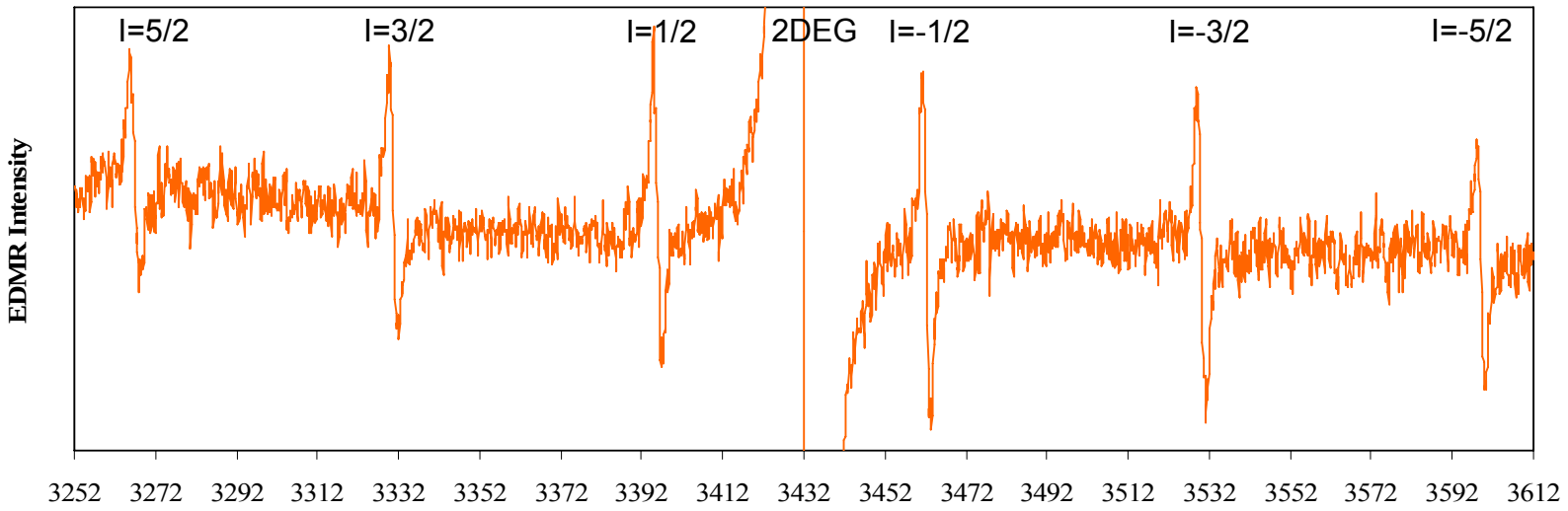

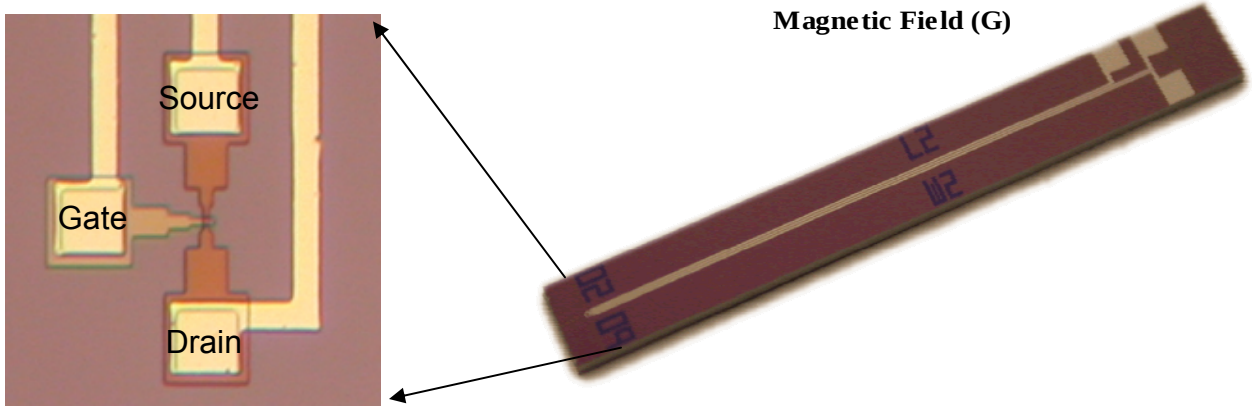

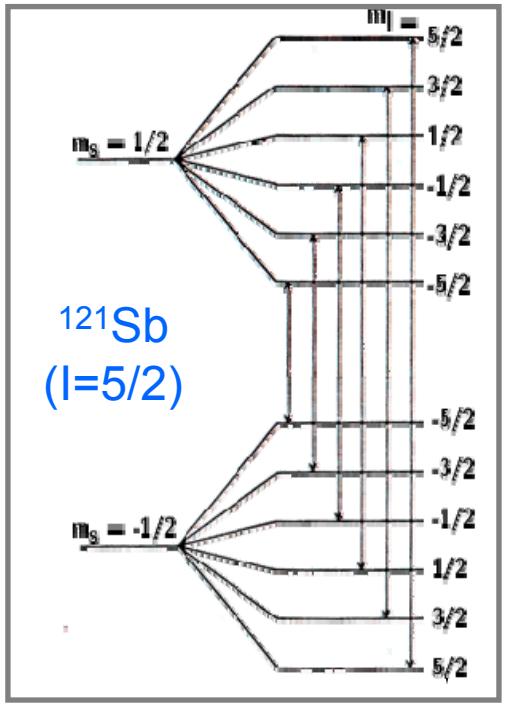

- Spin Dependent Transport characterized by Electrical Detection of Magnetic Resonance (EDMR) in transistors formed in ^{28}Si with implanted ^{121}Sb donors. Signal from ~10^6 donors in a 20x160 μm device. From line width of ~1.5 G, we can estimate T_1>30 ns.
- **C. C. Lo, et al., Appl. Phys. Lett. (2007)**
- systematic studies vs. gate bias and microwave power show that this is from neutral donor scattering, not from microwave heating
- **smallest device showing EDMR to date: 5x20 μm²**

M. Sarovar, K. C. Young, T. Schenkel, K. B. Whaley, Phys. Rev. B 78, 245302 (2008)
QND readout via EDMR

1. Transfer quantum state information from donor electron (in pure initial state) to nuclear spin (in mixed initial state)

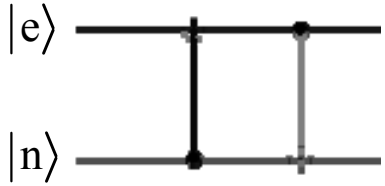

$$\mathrm{TRANS}=\mathrm{CNOT}_e \cdot \mathrm{CNOT}_n$$

Implement CNOT gates by on resonant pi-pulses between states:

1st: π – pulse at ω_e (MW)

2nd: π – pulse at ω_n (RF)

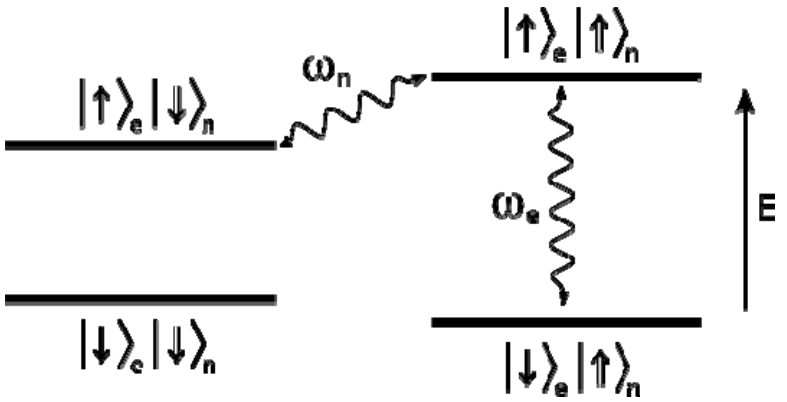

State of one spin only switched if other spin"points up"

$$|\Psi_e\rangle = \alpha|\uparrow\rangle_e + \beta|\downarrow\rangle_e$$

Applying TRANS gate and then tracing out conduction electron spin (not measured) shows that electron state information now resides in nuclear spin populations

$$\mathrm{Tr}_e\left(\mathrm{TRANS}_e\left[\rho_e \otimes \tau_n\right]\mathrm{TRANS}_e^{\dagger}\right) = \begin{pmatrix} |\alpha|^2 & \alpha\beta^*(w+w^*) \\ \alpha^*\beta(w+w^*) & |\beta|^2 \end{pmatrix}$$

2. Readout for single donor nuclear spin by EDMR

- Donor nuclear spin population measured by presence/absence of spectral line
- Need to measure before nuclear spin flips, i.e., within T_1 of nucleus
- Repeat entire procedure $\rightarrow$ get values of α and β for electron spin qubit with correct statistics

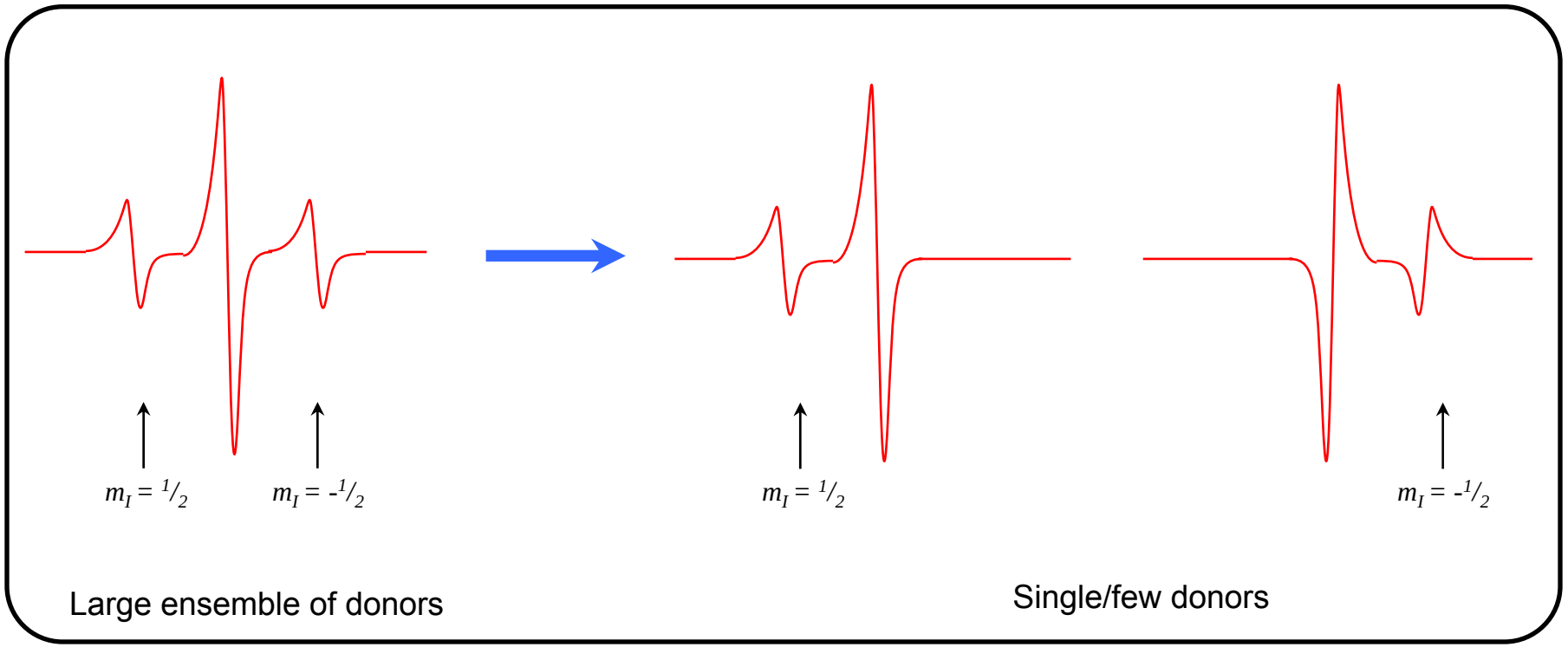

3. Feasibility of this qubit readout protocol:

- solve for steady state solution of donor spin → equilibrium spin value and hence single donor differential EDMR current

$$\frac{\Delta I}{I_0} \equiv \frac{I-I_0}{I_0} \approx -\alpha' \; s \; < \sigma_z >_i^{SS} \; P_c^0 \frac{1/\tau_n}{1/\tau_t} \qquad \text{with} \quad \alpha' \equiv \langle \Sigma_s - \Sigma_t \rangle|_{z=z_i} / \langle \Sigma_s + 3\Sigma_t \rangle|_{z=z_i}$$

- scale down to single donor measurement with improvements in
  - Scattering rate ratio: increase by
    - reducing 2DEG area as donor density decreases
    - improve channel mobility
  - Conduction band polarization: increase by
    - using spin injection
    - measure at higher magnetic fields
- estimate shot-noise limited measurement time $\tau_m \sim 10^{-3}$ s
- at T~ 1K, B > 1T, estimate nuclear T_1 under driving much larger than τ_m (recently confirmed by Princeton group)

$$\frac{\Delta I}{I_0} = 10^{-4}$$

$\Rightarrow$ 100 nm-scale transistor for single donor qubit state measurement

Test with 100 nm scale devices are in progress, …

aFET4 – SOI (FinFET)

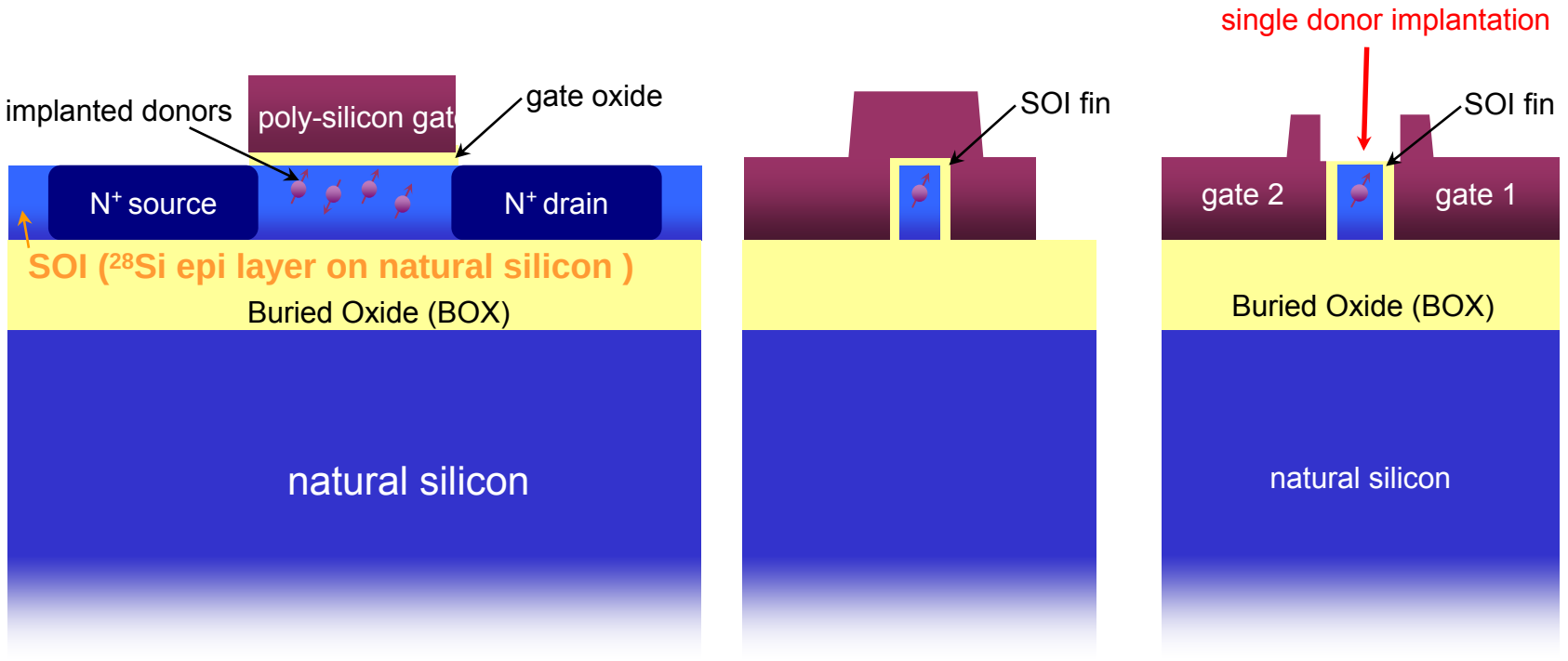

- ^{28}Si epi on ^{nat}Si SOI Fins
- Single-ion implant compatible
- Improved contacts
- e-beam lithography scaling to 50 nm scale devices with 1 to 10 donors in the channel

Example of Random Telegraph Noise tuning close to the gate threshold bias in 100 nm scale FinFets at 4 K (V_{SD}=50 mV)

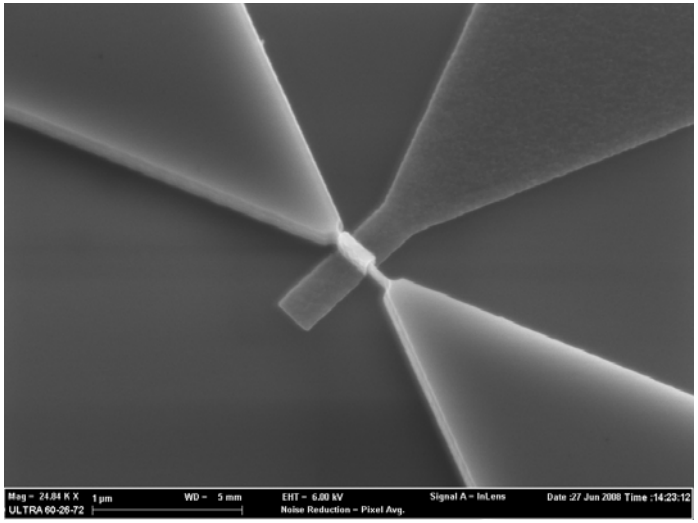

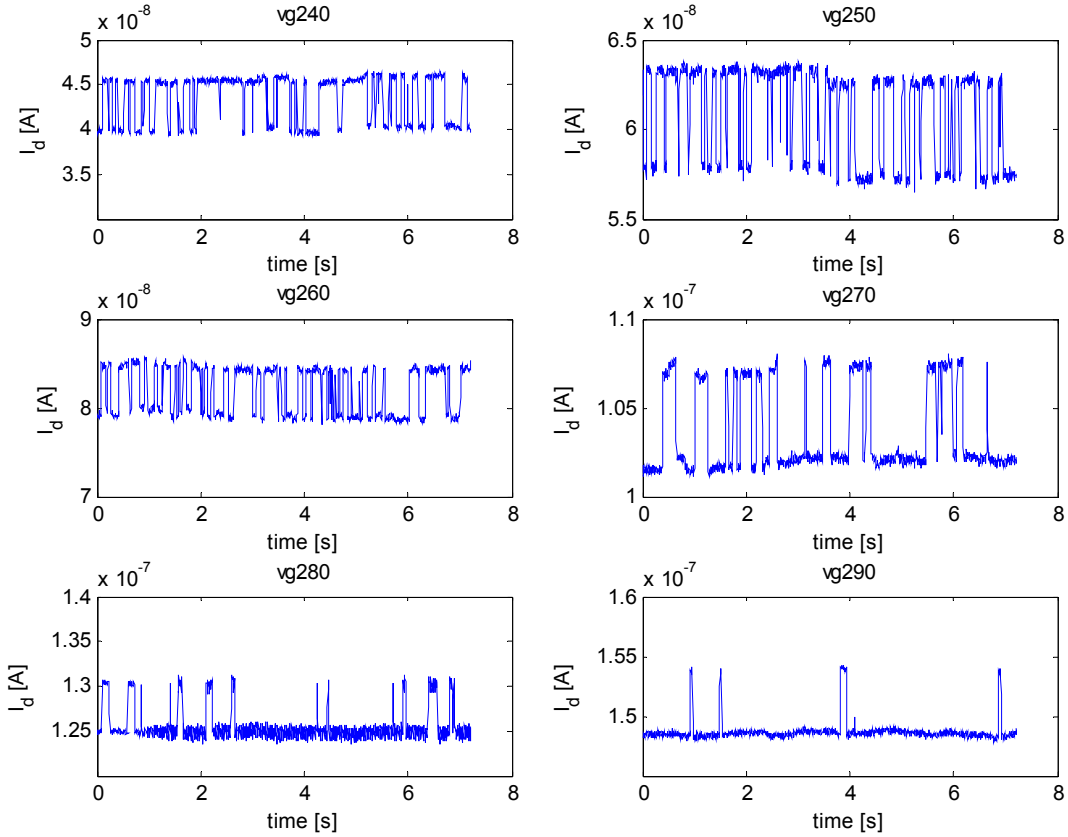

Above threshold: e. g. FinFet#0221, 300 x 150 nm. V_g = 400mV, I_{SD}=100nA, and V_{SD}=22mV, noise dR/R~8x10^{-5}.

FinFets with spin injection gates, first x-band EDMR data (in progress)

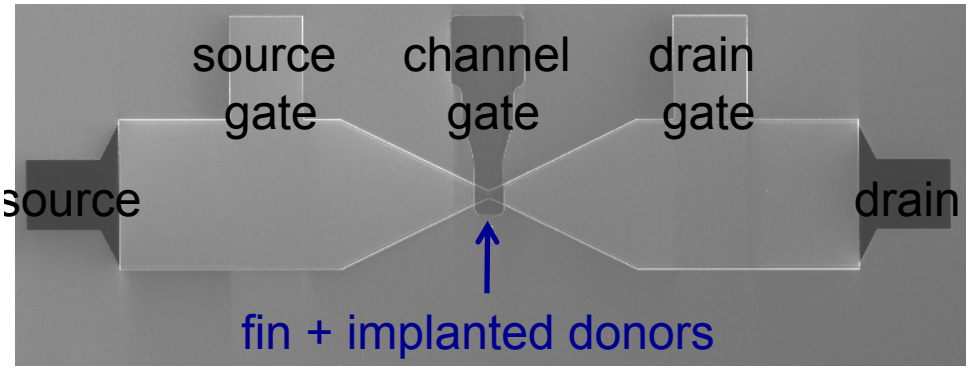

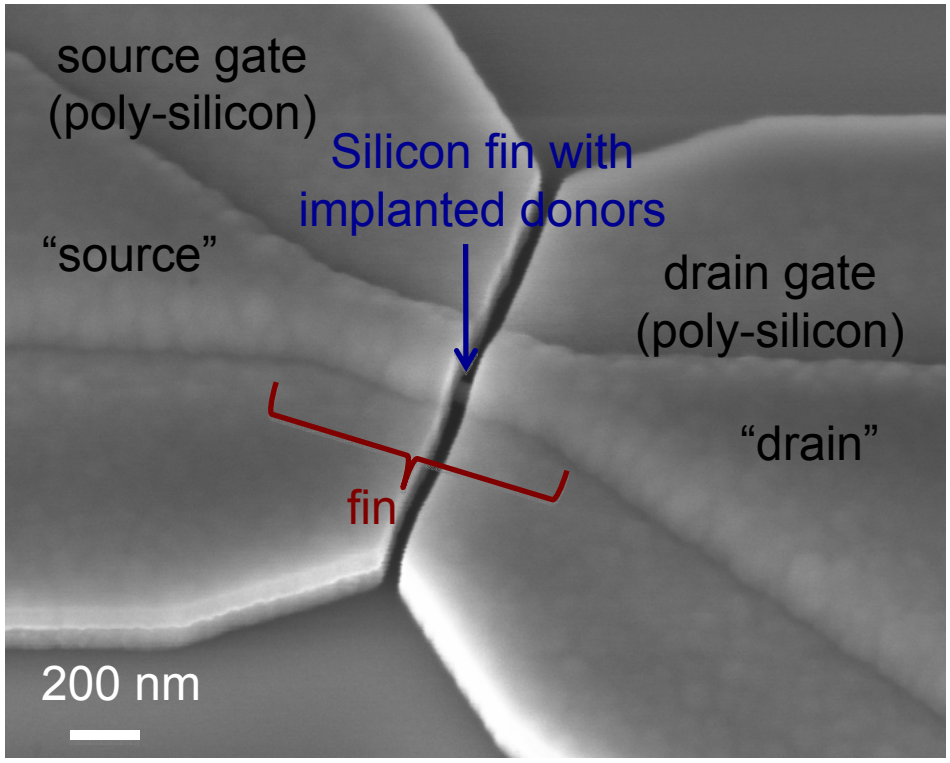

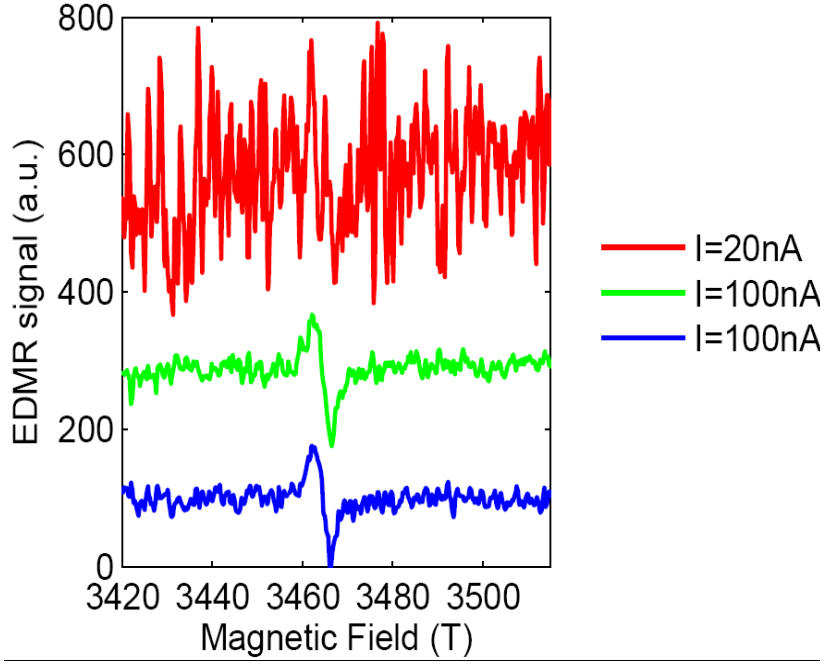

- 1st x-band EDMR data from FinFETs, 2DEG signal only (incl. some contribution form sides gates)
- side gates enable future implementation of spin injection contacts without inducing large inhomogeneous broadening
- side gates eliminate random donor in-diffusion from n+ doped contact regions into the channel, enabling ultra-short channels
- single donors in scaled FinFet channels approximate tunable quantum dots

Doping in these devices predicted to allow single nuclear spin state sensing

1. Introduction

2. Spin readout transistors

3. Single Atom Doping

4. Outlook

Beating Poissonian distributions of implanted ions by single ion detection

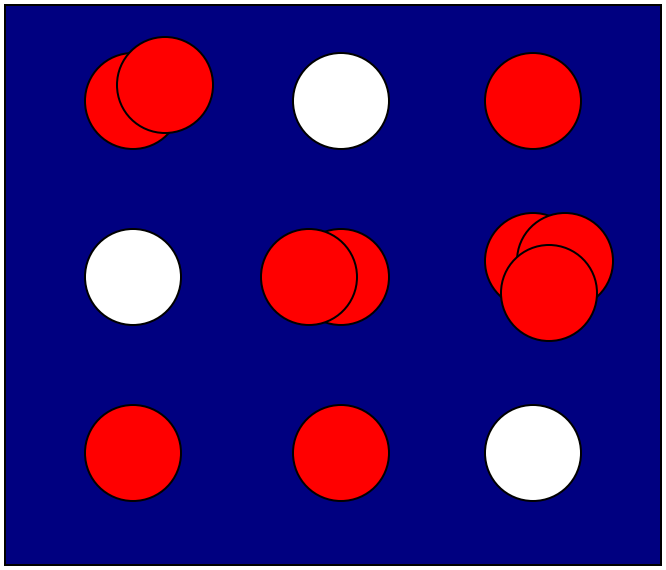

- Distribution of probabilities for implantation of ions where the implantation probability is small (<<1) for each incident ion and the number of ion impacts is large (>>1)
- At average, one ion is implanted. The probability for two adjacent ion hits is 13%

Placement Accuracy in Single Atom Doping

Δx = spot size + straggling + diffusion

Δx << qubit spacing

qubit spacing e. g. 10 to 20 nm, but depends on coupling scheme

Spin qubit coupling
- via J or magnetic dipolar coupling (nearest neighbor)
- via coherent electron shuttling
- via cavity coupling
- via spin to photon, photon to spin conversion
- …

Ion implant setup with scanning probe alignment and three ion sources

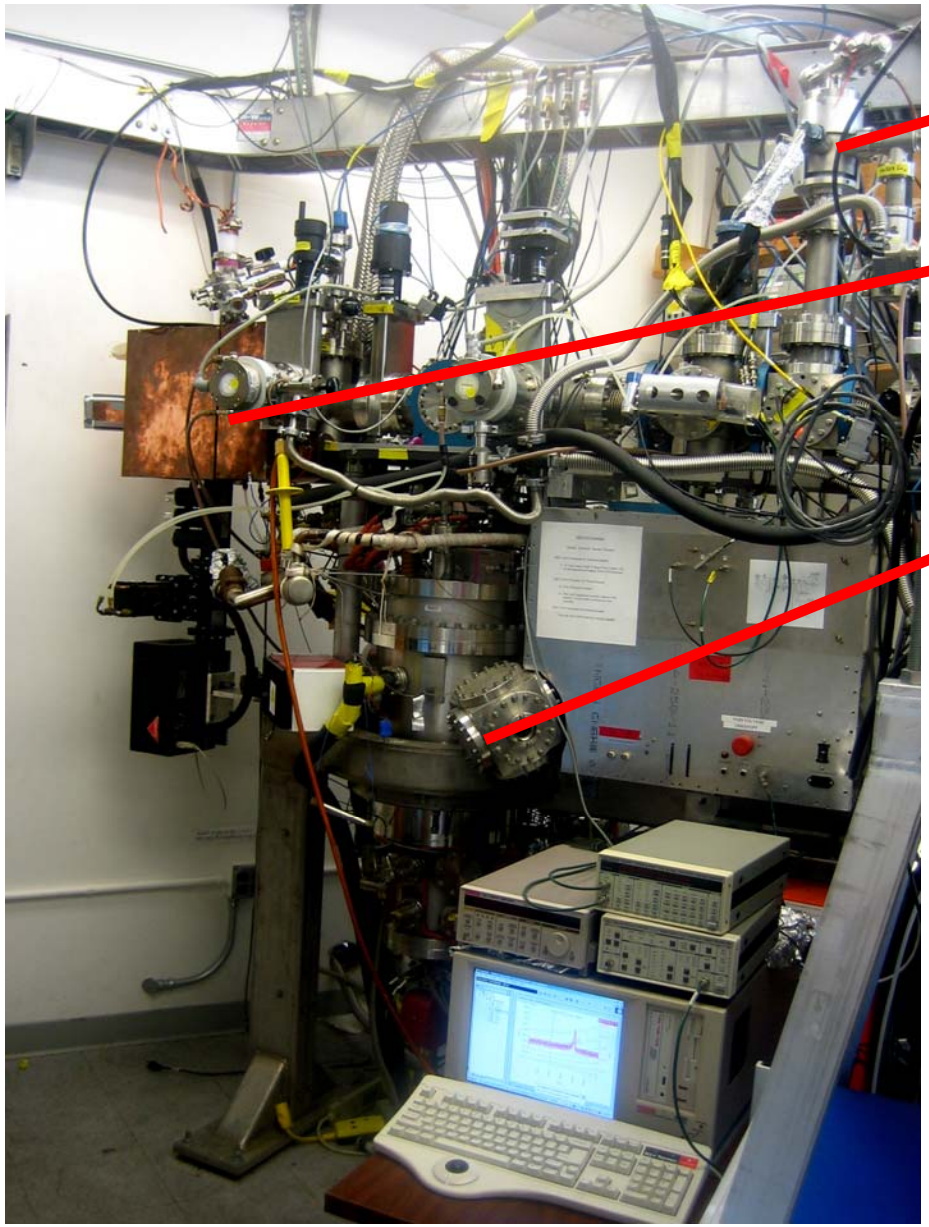

1. **Low density plasma source** for low ion charge states and molecular ions, e. g. $^{15}N_2^+$, Ar[1 to 3+], 1 to 15 keV
2. **ECR (Electron Cyclotron Resonance Source**), driven with 2.5 GHz micro waves for low to medium ion charge states, e. g. Sb [3 to10+], 3 to 150 keV
3. **EBIT (Electron Beam Ion Trap)** for medium to high ion charge states, e. g. Sb [4 to 40+], 10 to 500 keV

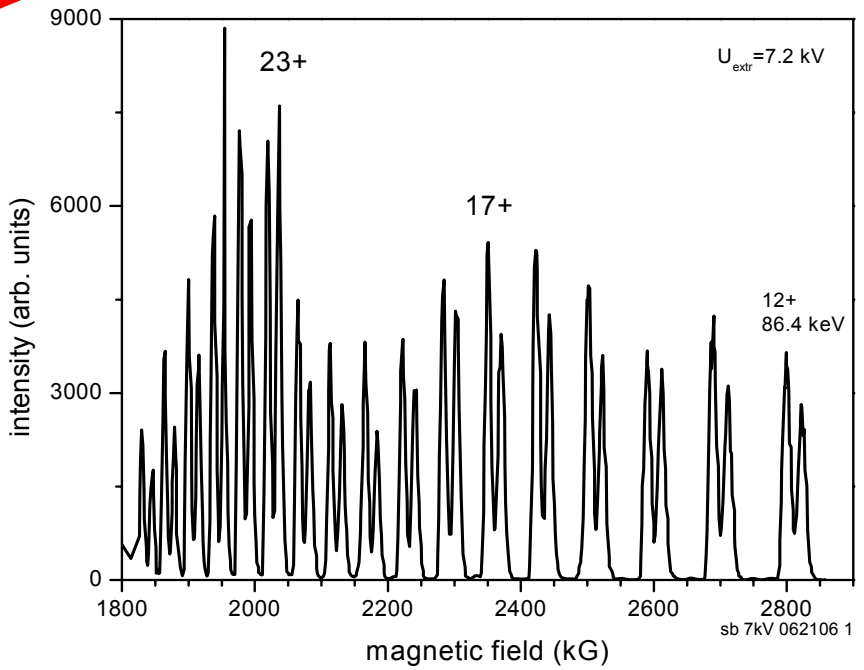

Setup for Ion Implantation with Scanning Probe Alignment

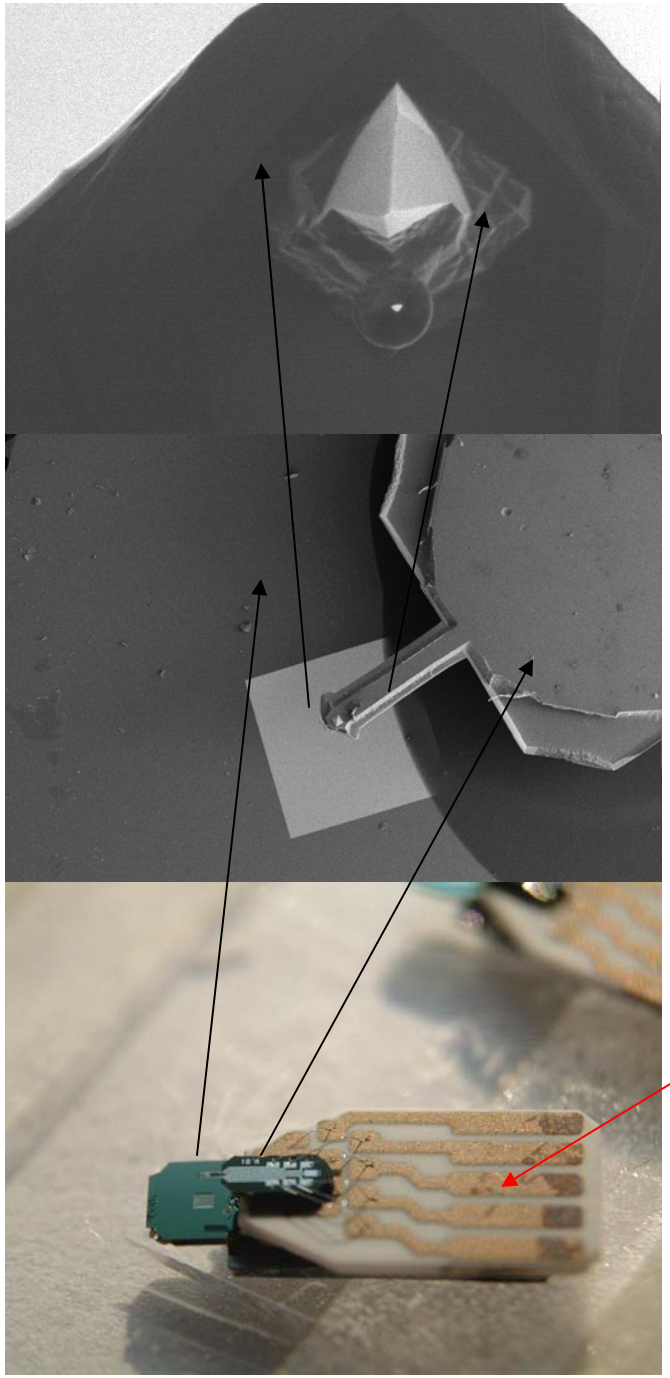

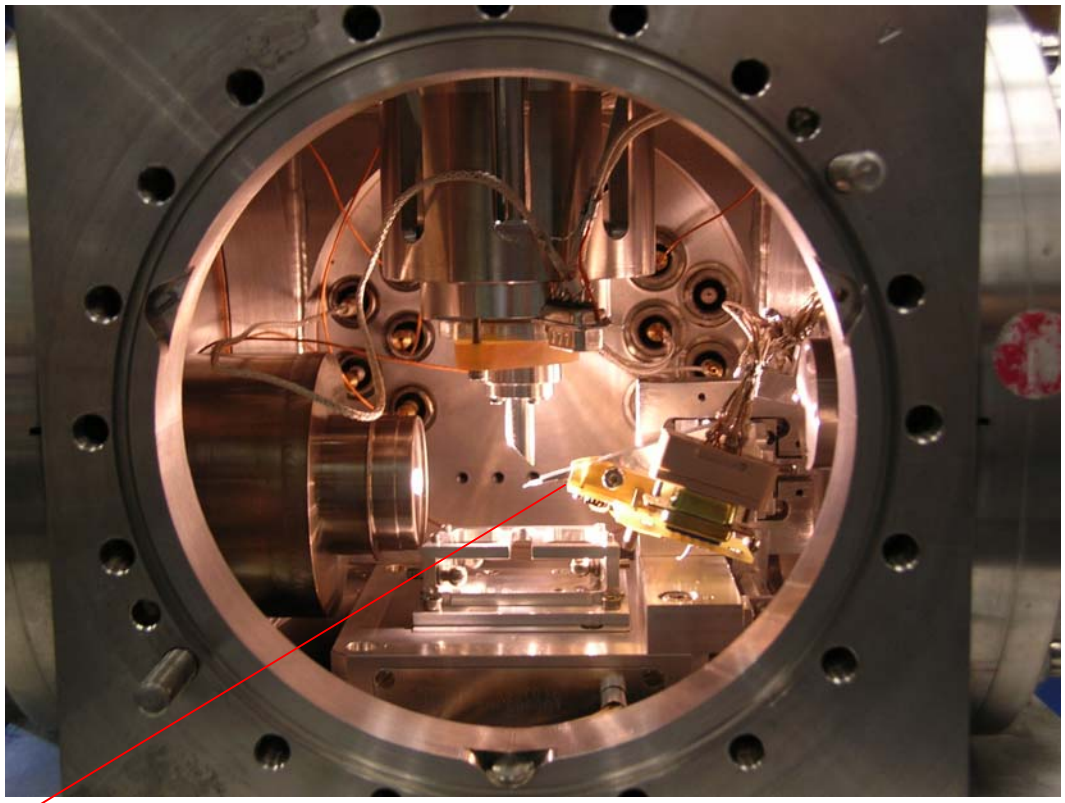

- Single Ion Implantation with Scanning Probe setup connected to high vacuum beam line
- scan range of target stage is 0.1 x 0.1 mm^2
- probe tip can be moved across 1 mm field
- piezo-cantilevers co. I. Rangelow, University Ilmenau
- holes down to <5 nm diameters by FIB processing

Single Ion Placement with Scanning Probe Alignment

- Non-destructive imaging and nm-apertures for nm-accuracy

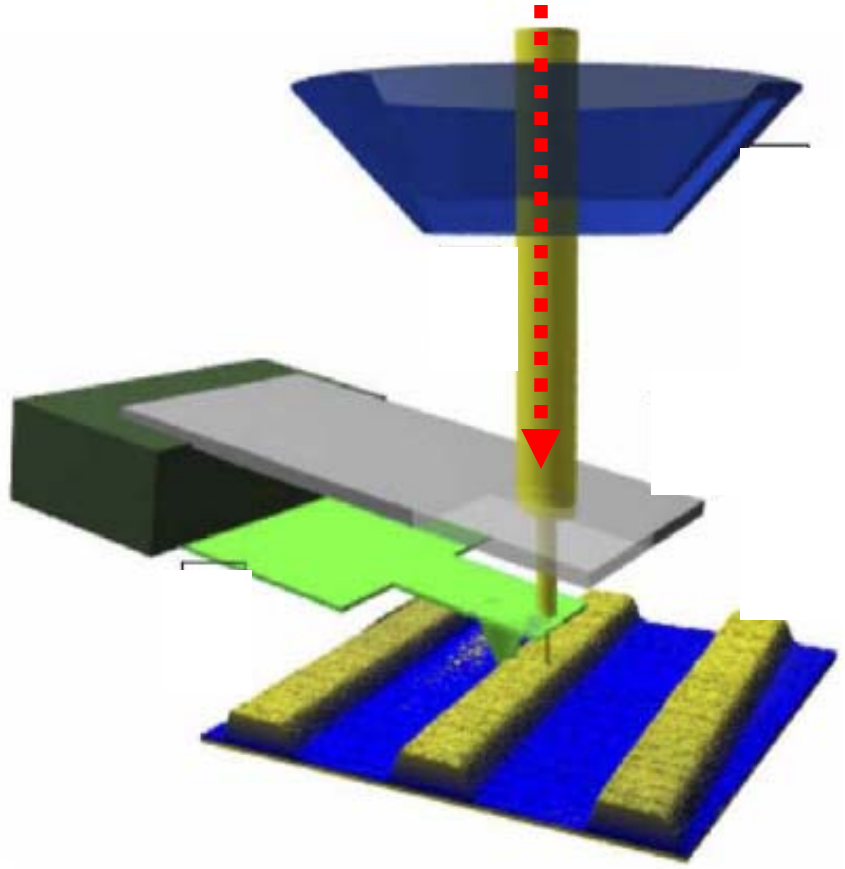

A. Persaud, et al.,
Nano Letters 5, 1087 (2005)

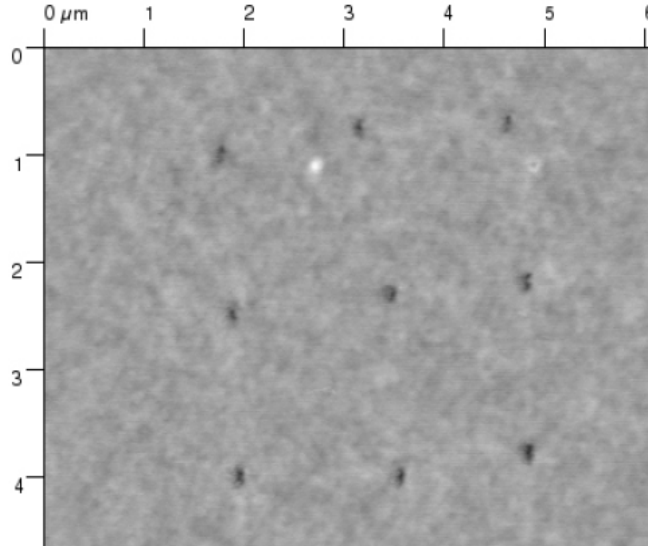

array of 90 nm dots in PMMA from ion implantation with scanning probe alignment

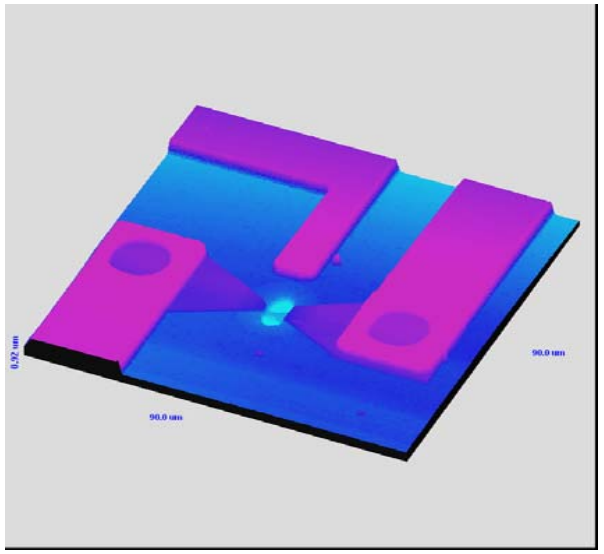

in situ scanning probe image of a FinFet

Setup for Ion Implantation with Scanning Probe Alignment

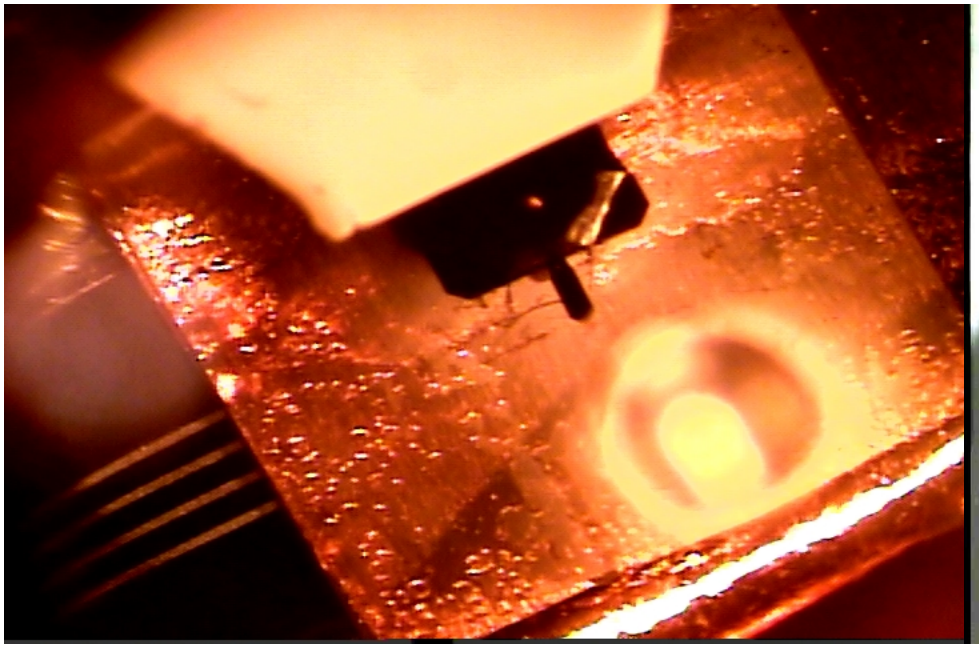

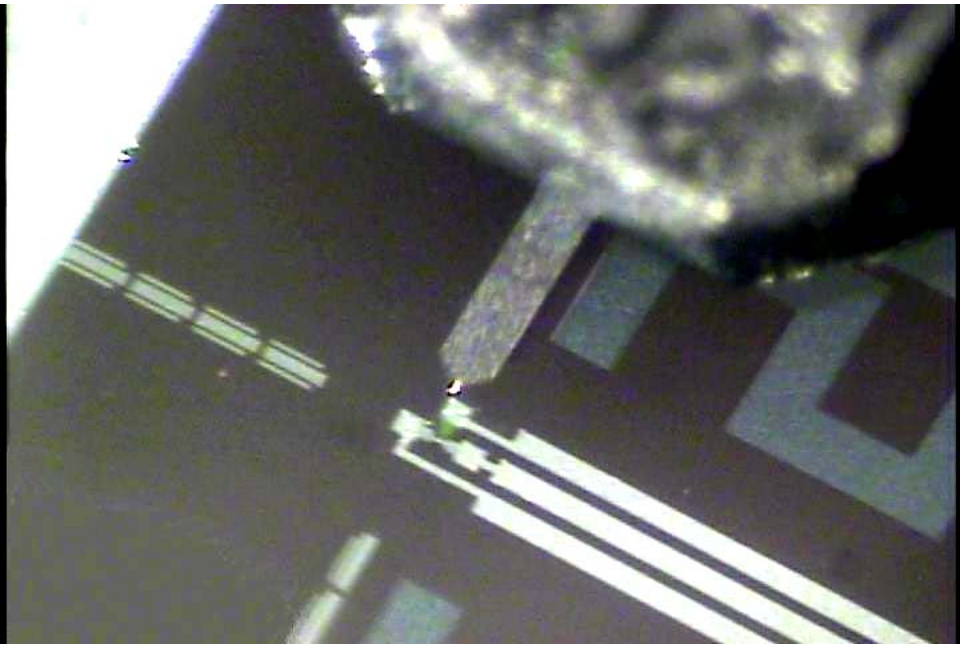

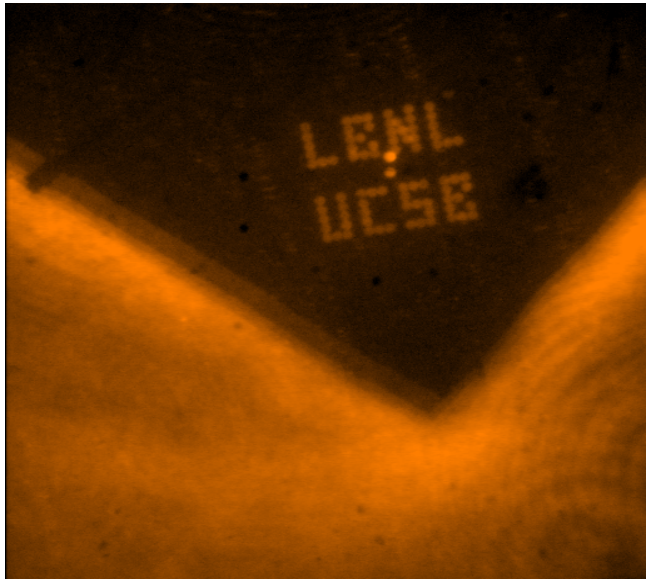

- **Scanning force microscope cantilever imaging a diamond sample (left) and a Field effect Transistor (right) for aligned (single) ion implantation**
- **bottom left: Photoluminescence from patterned NV-centers in diamond (co. E. Sideras-Haddad and D. Awschalom, UCSB)**

Single Ion Detection in Readout Transistors through ion impact induced current changes

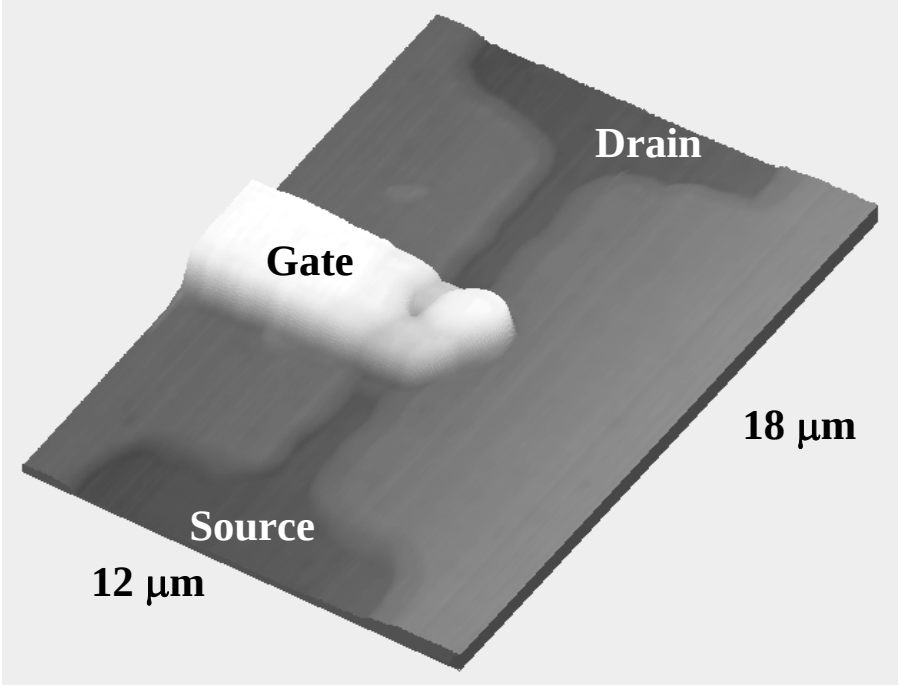

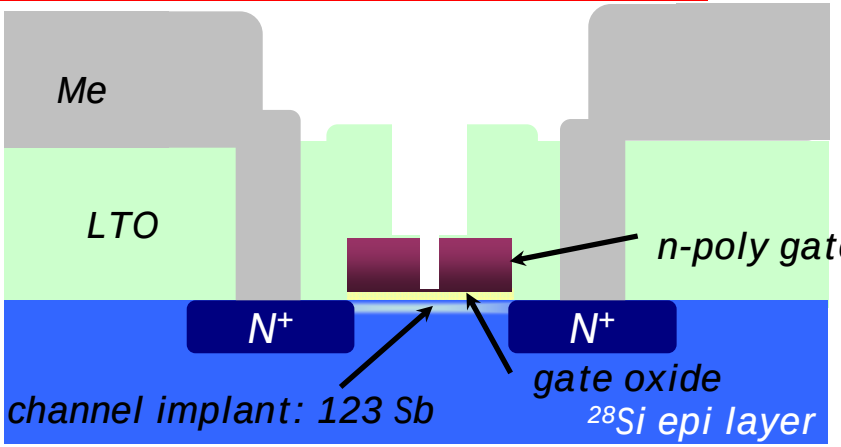

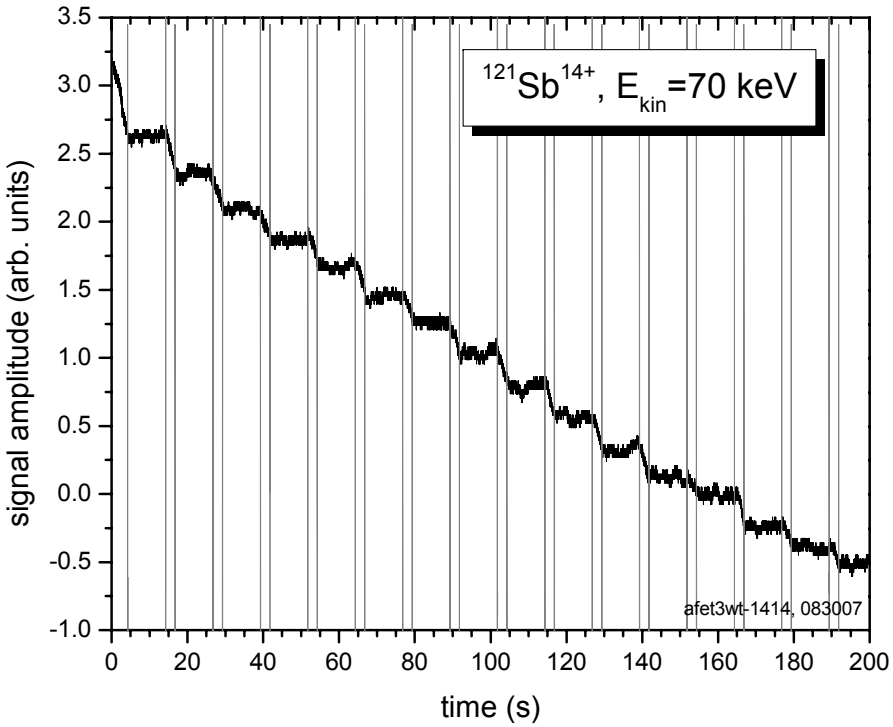

• single ion doping through detection of current transients from single ion impacts (dI~ few 10^{-4} dI/I, in 2x2 μm aFets at room temperature)

Last year: Single Ion Detection in Readout Transistors through ion impact induced current changes

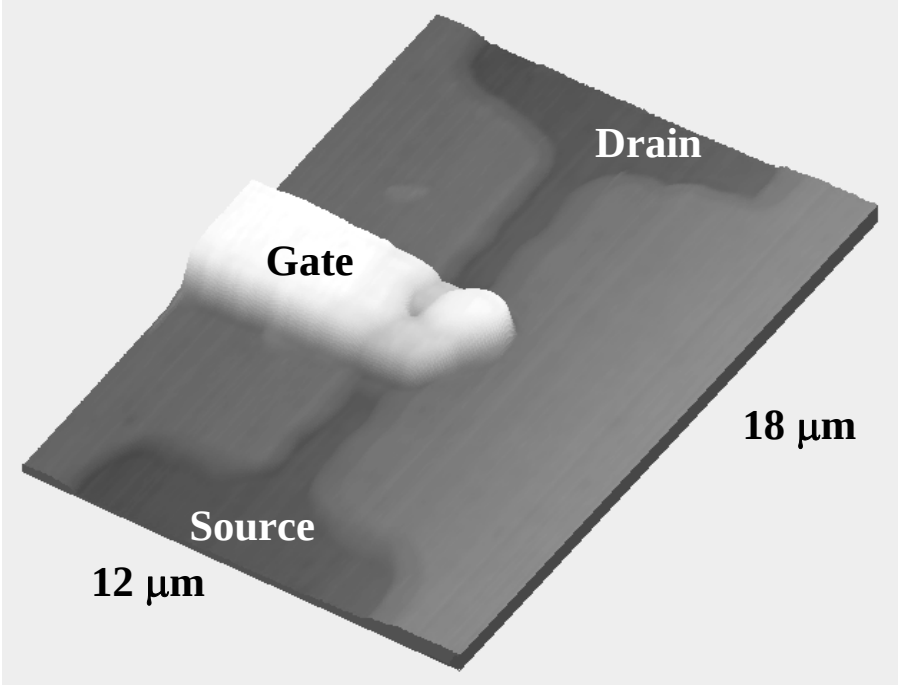

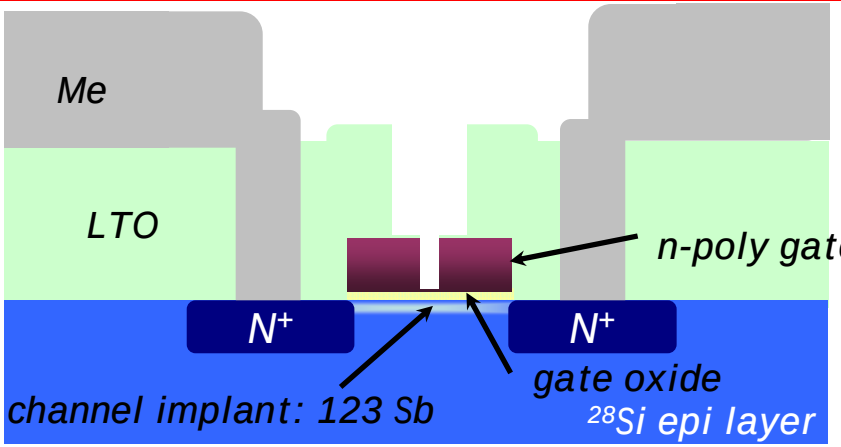

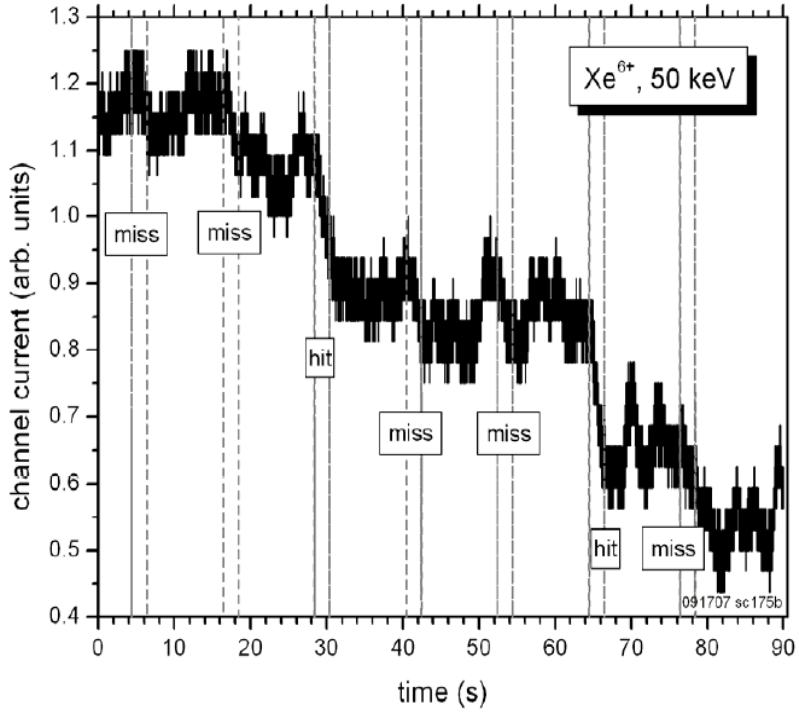

• single ion doping through detection of current transients from single ion impacts (dI~ few 10^{-4} dI/I, in 2x2 μm aFets)

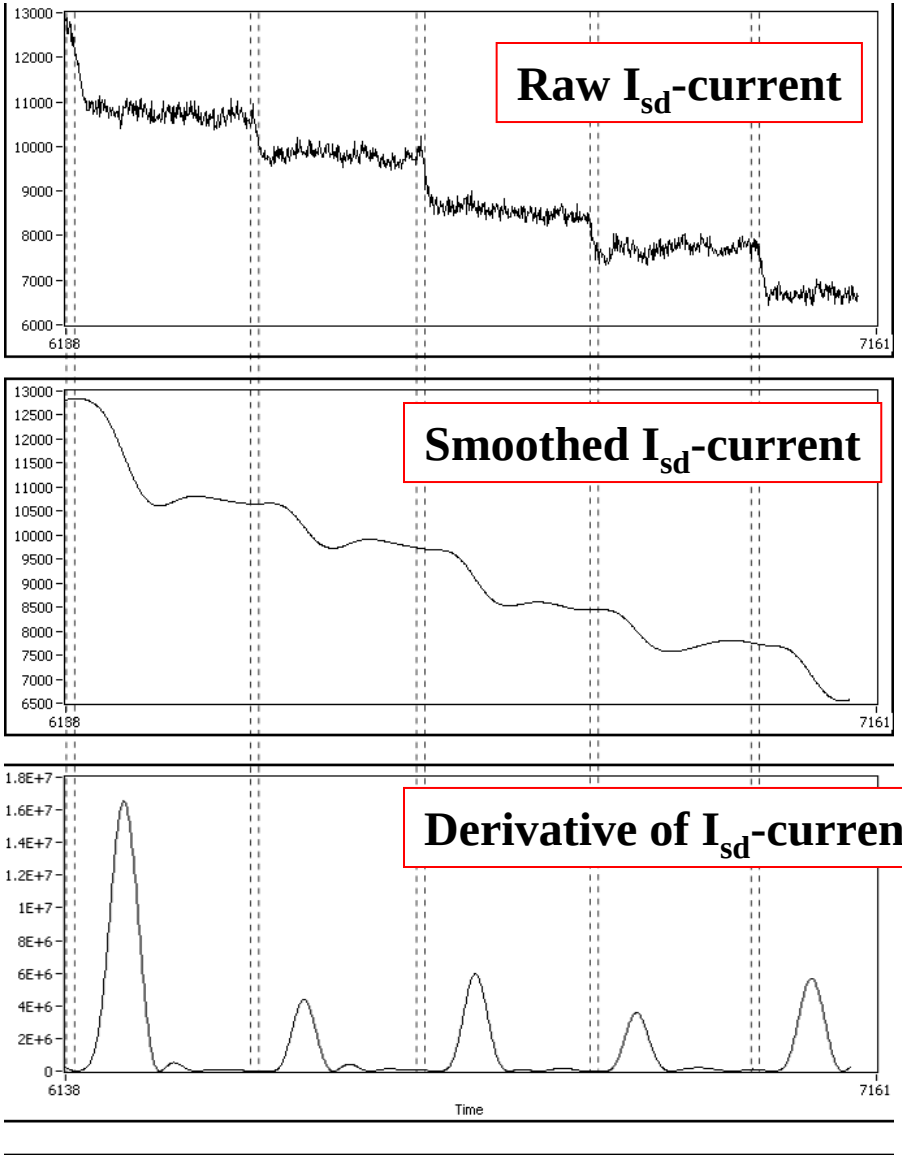

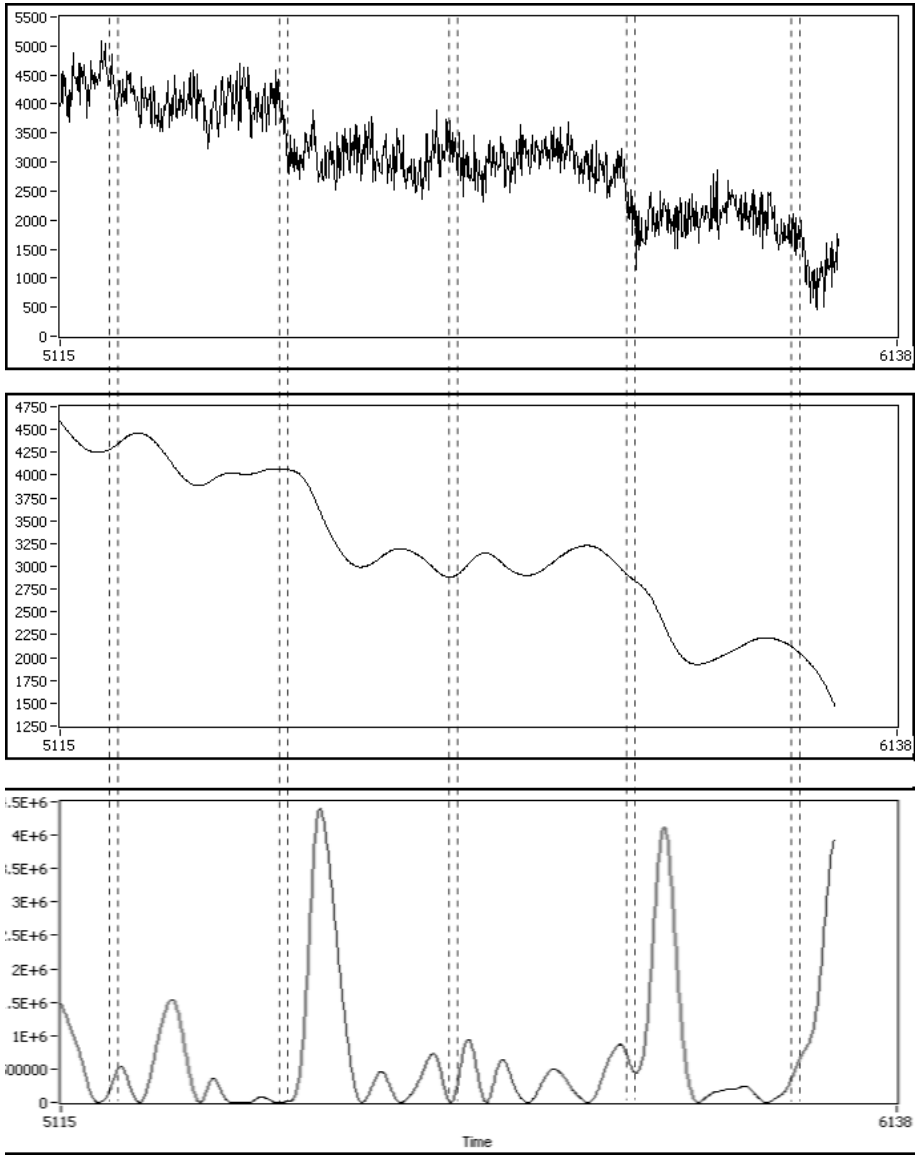

Hits for every pulse = multiple ions per pulse

Hits and misses ≅ single ions per pulse

Large single ion impact signals at room temperature with 100 nm scale FinFets

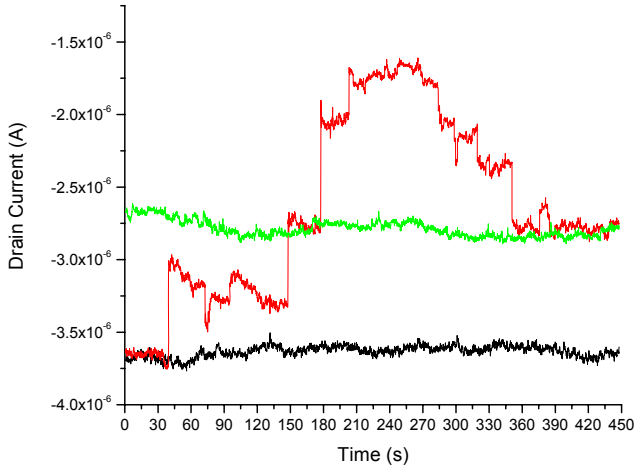

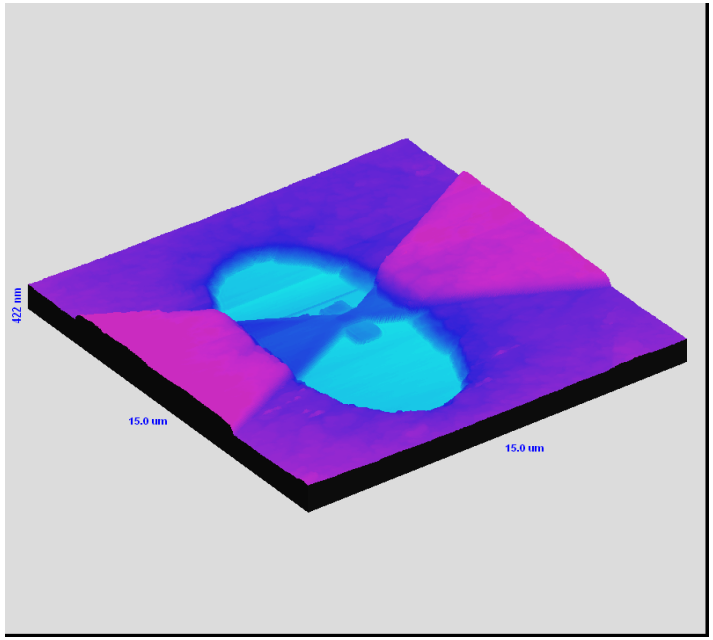

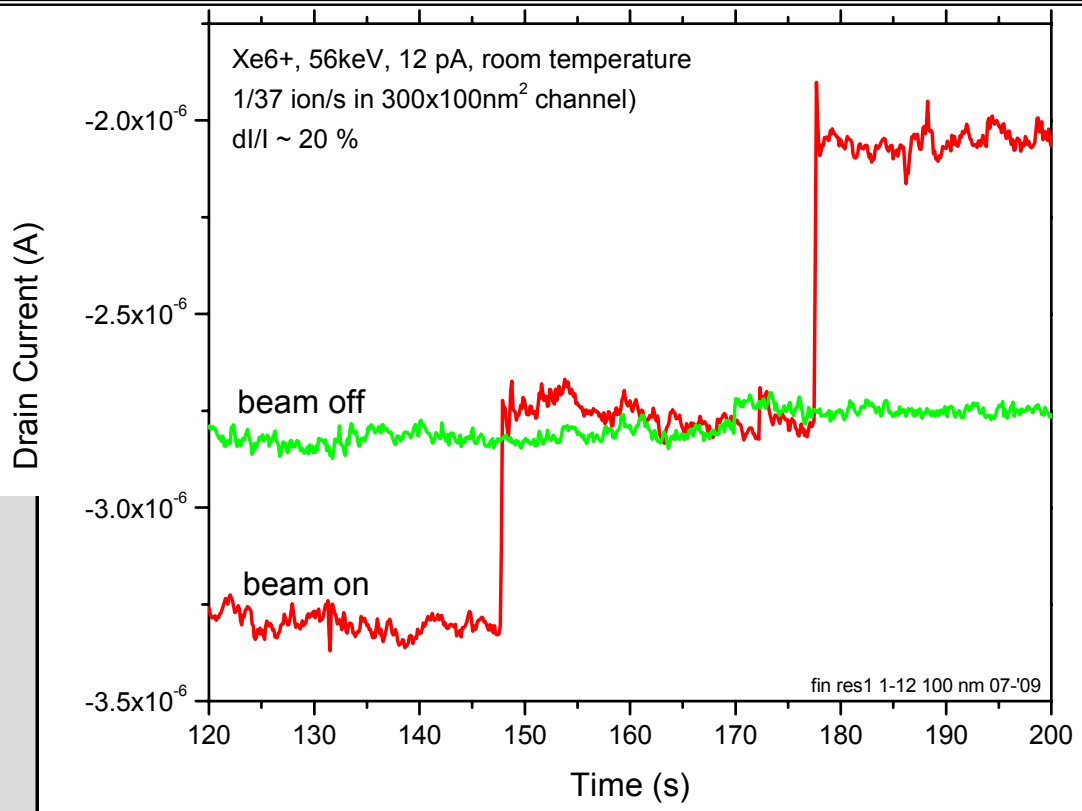

Left: in situ scanning probe image of FinFet structure
Top left: Fet source-drain current modulation over time during single ion implantation
Right: Single ion impact signals from a FinFet at room temperature

Spatially resolved, *in situ* monitoring of (single) ion implantation

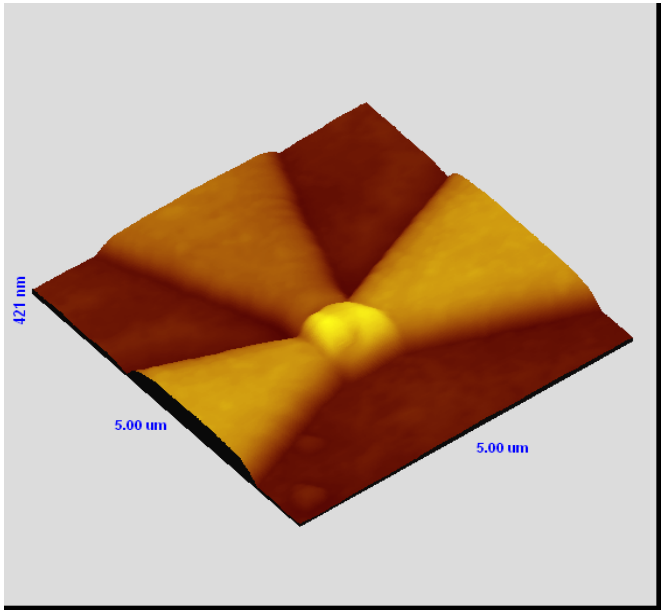

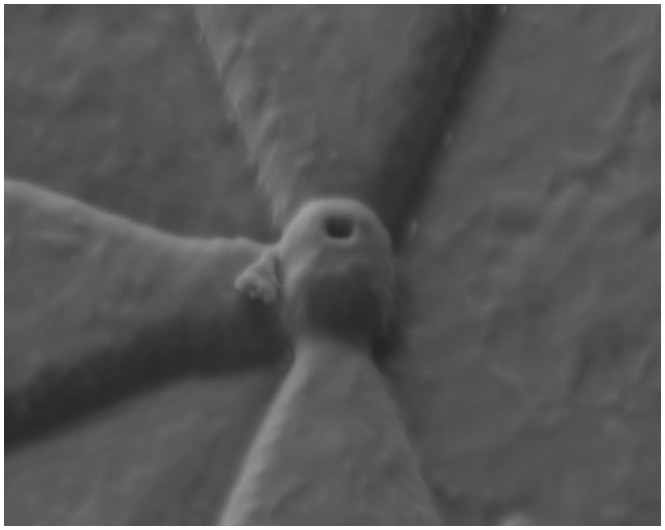

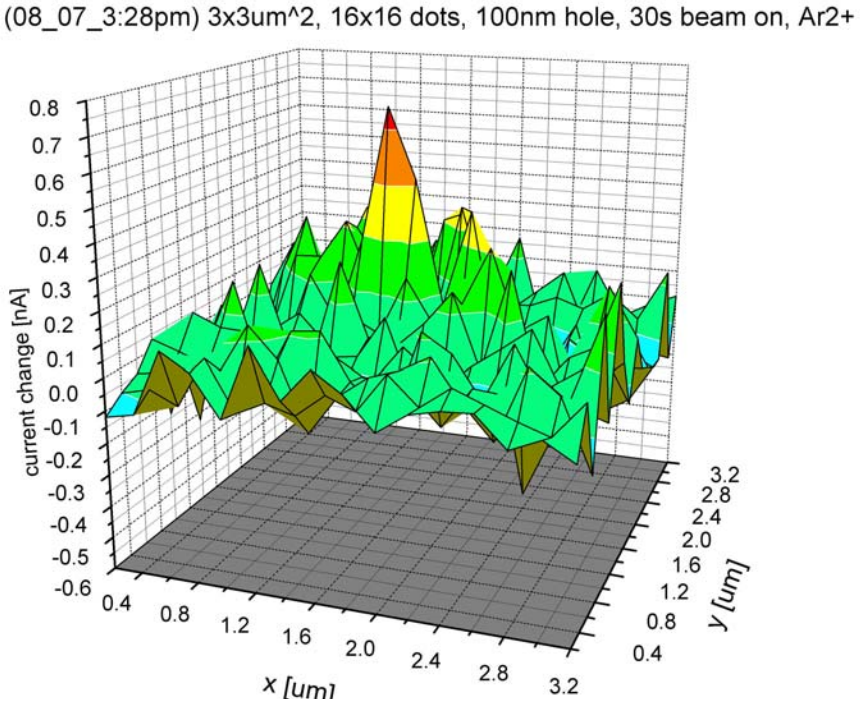

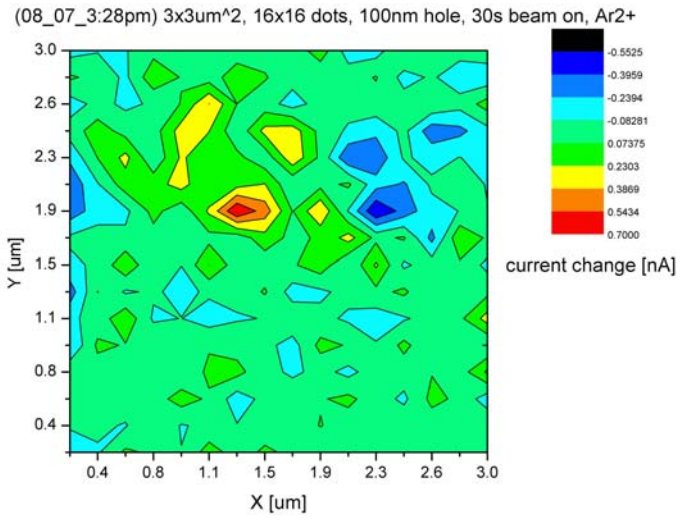

Poly and Tungsten electrodes allow annealing post single ion implantation of readout transistors, enabling iterative cycles of single ion doping and device characterization

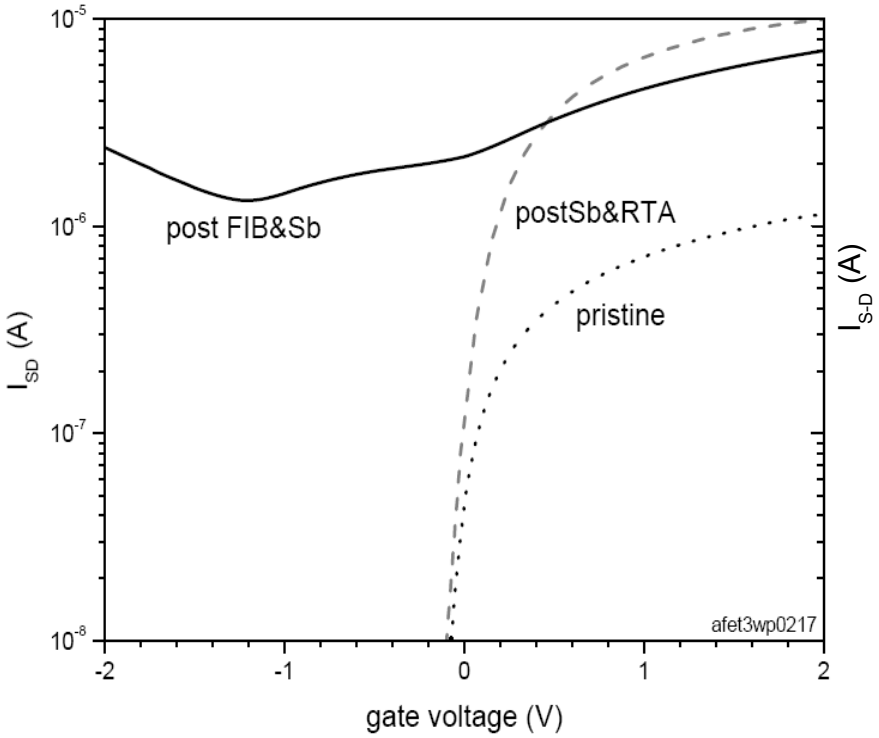

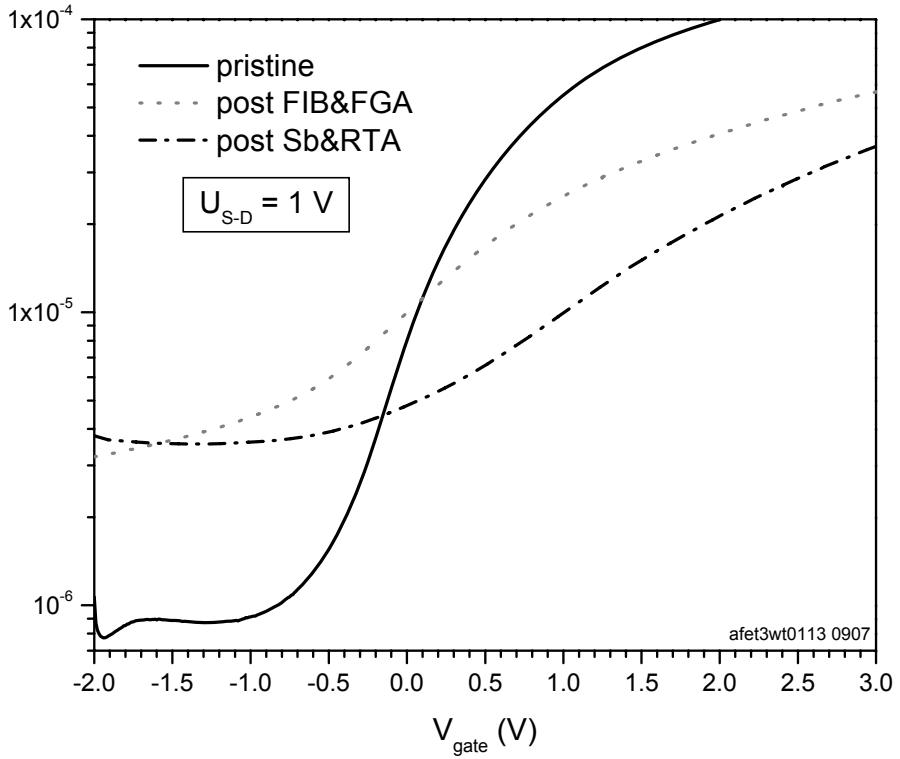

-I-V for an nFet3 (n+/p/n+), Fib induced leakage is eliminated in the post-implant annealing step

-I-V for an aFet3 (n+/n/n+), Fib induced leakage reduced, but on-current also down following implant annealing step, studies of mechanisms in progress

Ultimate limit in dopant placement by implantation ?

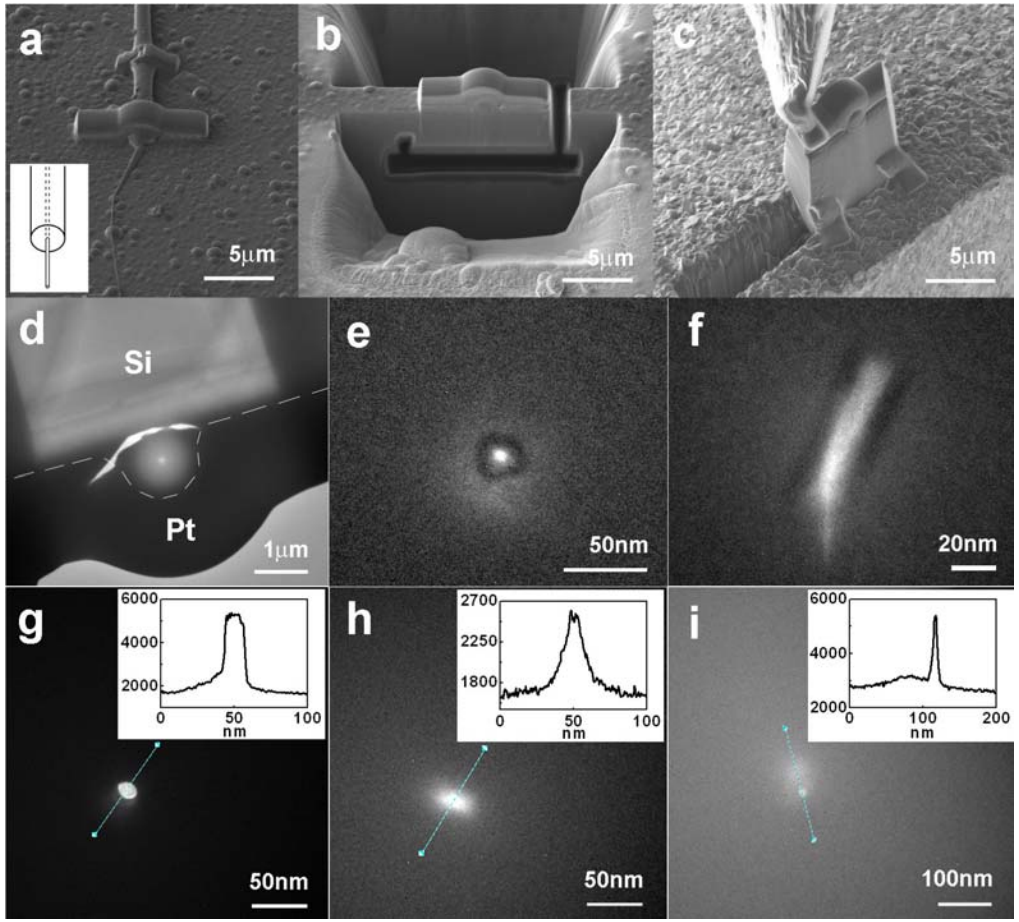

- Straggling:
  - •minimize with low energy and high Z, can get <5 nm
- Diffusion / Segregation
  - Sb stays put (D_0~6×10^{-15} cm^2/s)
- Spot size for CNTs ~ 1 – 10 nm

→few nm placement accuracy is possible !

Electron transport through a single Carbon Nanotube (CNT)

G. Chai, H. Heinrich, T. Schenkel and L. Chow, *Appl. Phys. Lett. 91, 103101 (2007)*

• tests with ions in progress

Metrology of donor implantation and processing

- tracking dopant profiles during thermal processing, Sb shows minimal diffusion / segregation among shallow donors in silicon

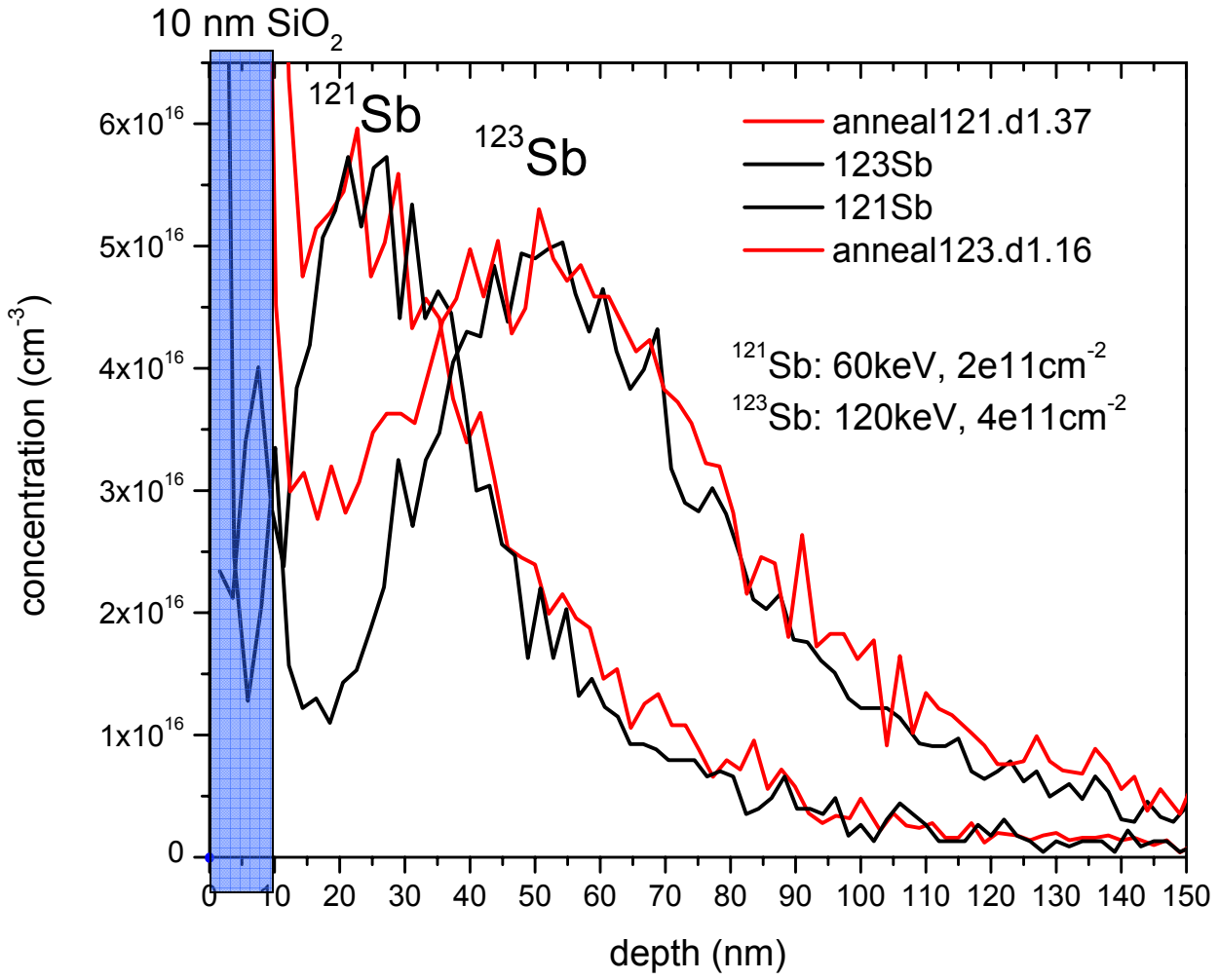

• SIMS depth profile of 121-Sb atoms as implanted and after annealing at 850º C for 10 s

1. Overview

2. Spin readout transistors

3. Single Atom Doping

4. Outlook

can we make use of long donor spin coherence times in scaled silicon devices?

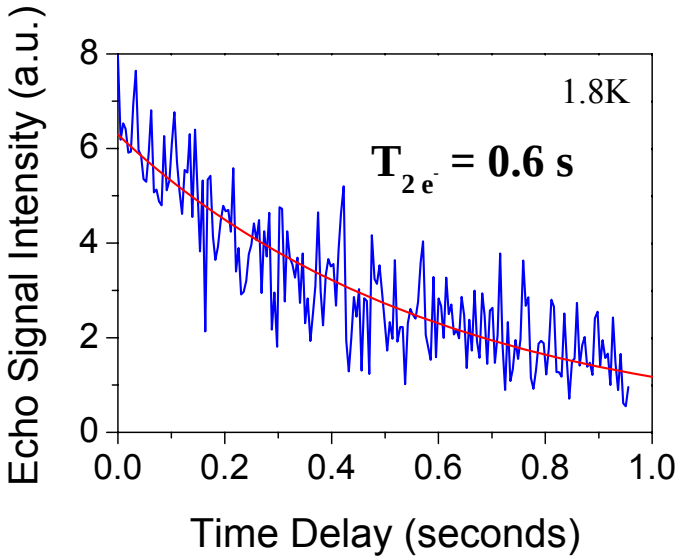

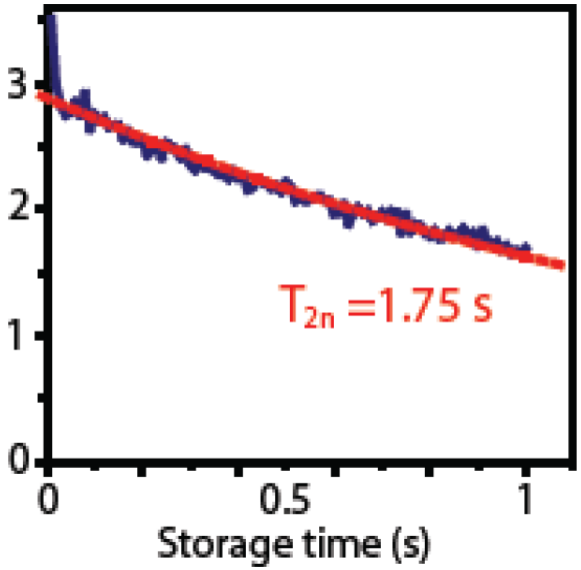

- Echo intensity for electron spins [top, Lyon et al., to be published], bottom, recovery amplitude vs. nuclear spin storage time for ^{31}P in ^{28}Si, J. Morton, A. Tyryshkin, R. Brown, S. Shamkar, B. Lovett, A. Ardavan, T. Schenkel, E. Haller, J. Ager, S. Lyon, Nature 455, 1085 (‘08)

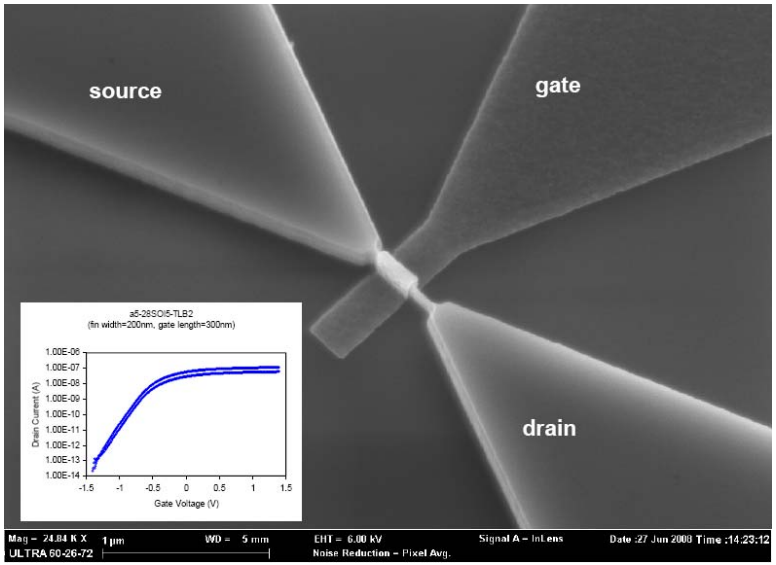

- 100 nm scale FinFet spin readout transistor formed in isotopically purified silicon on insulator (^{28}SOI) and implanted with ^{121}Sb. I_{sd}-V_g curves in the insert.

Spins in Diamond: NV^-, N

-NV center (1.95 eV) most popular right now, but has limitations

→ rational selection, testing and integration of optimal centers (e. g. SiV, NiV, …)

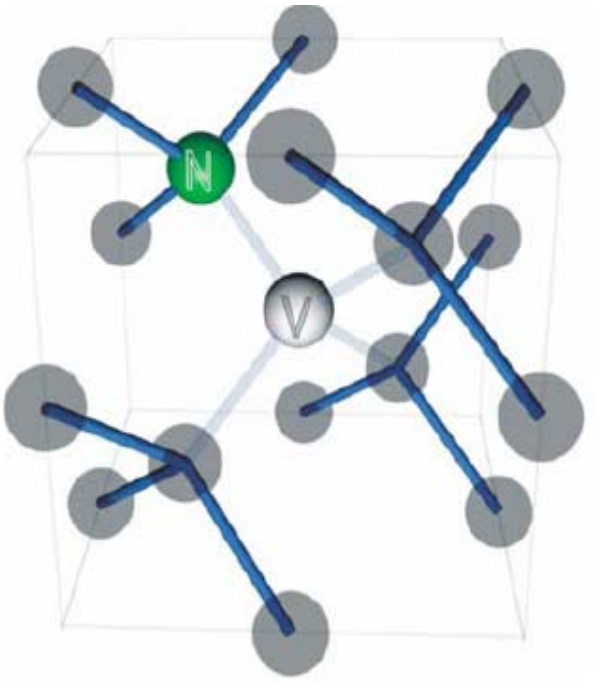

Wrachtrup Phys. Stat. Sol., 2006

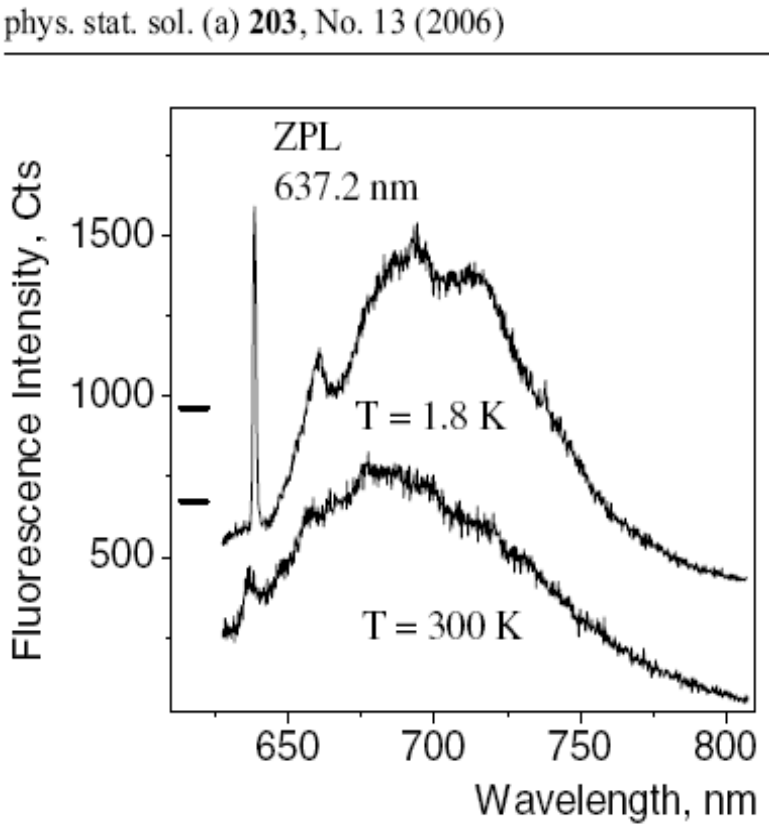

(Excitation was at 514 nm)

Electron spin – lattice relaxation time for Nitrogen donors in Diamond is about 1 ms at 300 K (at B = 0.3 to 8 T)

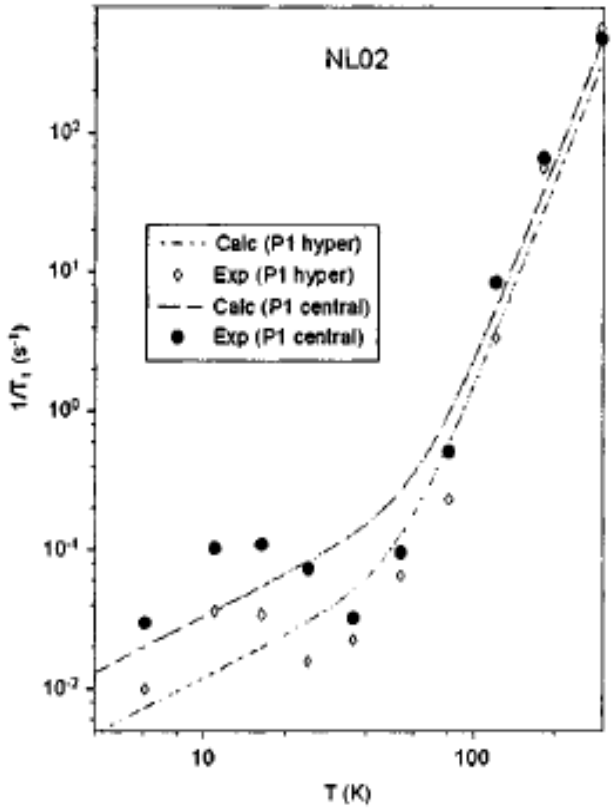

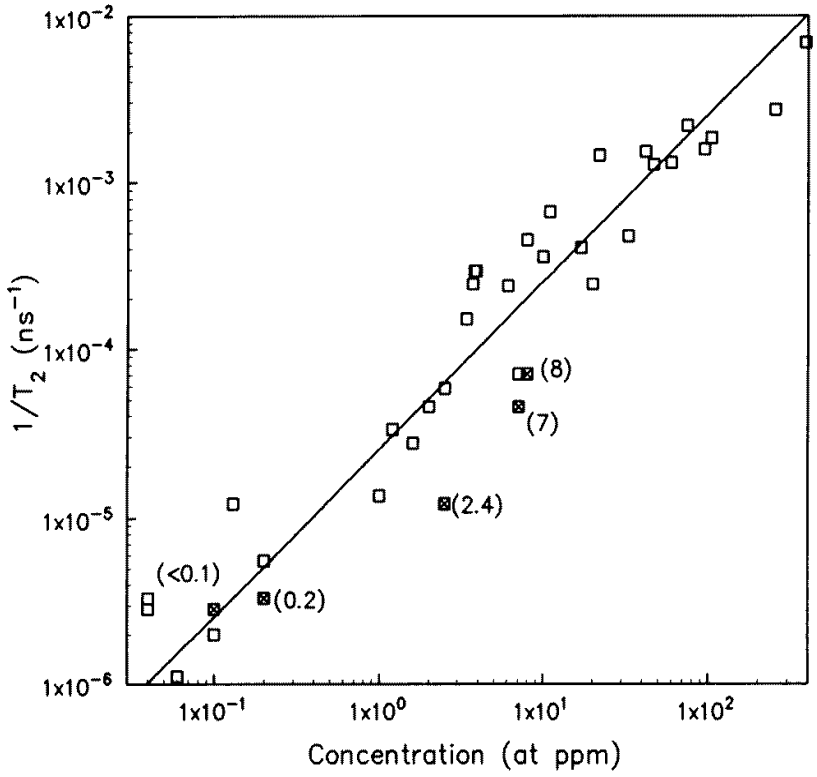

-rather independent of DC magnetic field since apparently dominated by spin-orbit phonon induced tunneling (van Wyk et co., J. Chem. Phys. '98; J. Phys. D 30 (1997) 1790)
- T2 limited by instantaneous diffusion, random dipole coupling between like spins (right) in natural diamond (1% ^{13}C) down to ~10 ppb (~1.7×10^{15} cm^{-3})

- Very long T1 and T2 at room temperature makes N and NV- exciting candidates for coupled spin dynamics studies in diamond. Coupling length scales are only a few nm, so this requires optimized single digit nanofabrication.

Formation of coupled NV-center arrays in ultra-pure diamond

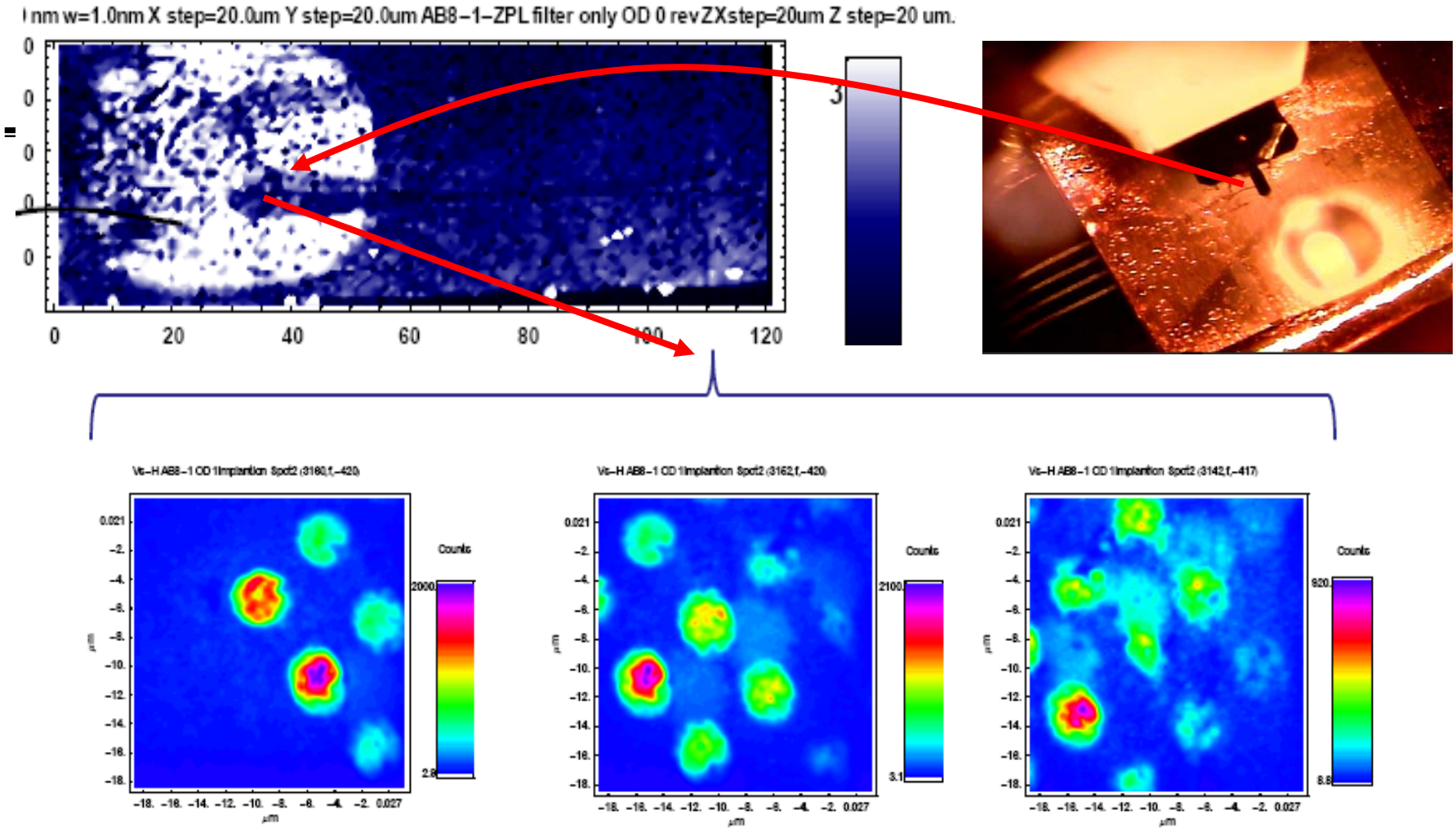

- implantation of low energy $^{15}N^{q+}$ and $^{15}N_2^+$ ions with scanning probe alignment and a series of implant doses
- isolated ^{15}NV centers have very long T_2's, >0.1 ms at room temperature, 1st μm-scale arrays
- **collaboration with G. Fuchs & D. Awschalom, UCSB, and E. Sideras-Haddad, Univ. Witwatersrand, Johannesburg,** arXiv:0806.2167, J. Vac. Sci. Technol. B, in press

Nitrogen implantation into diamond

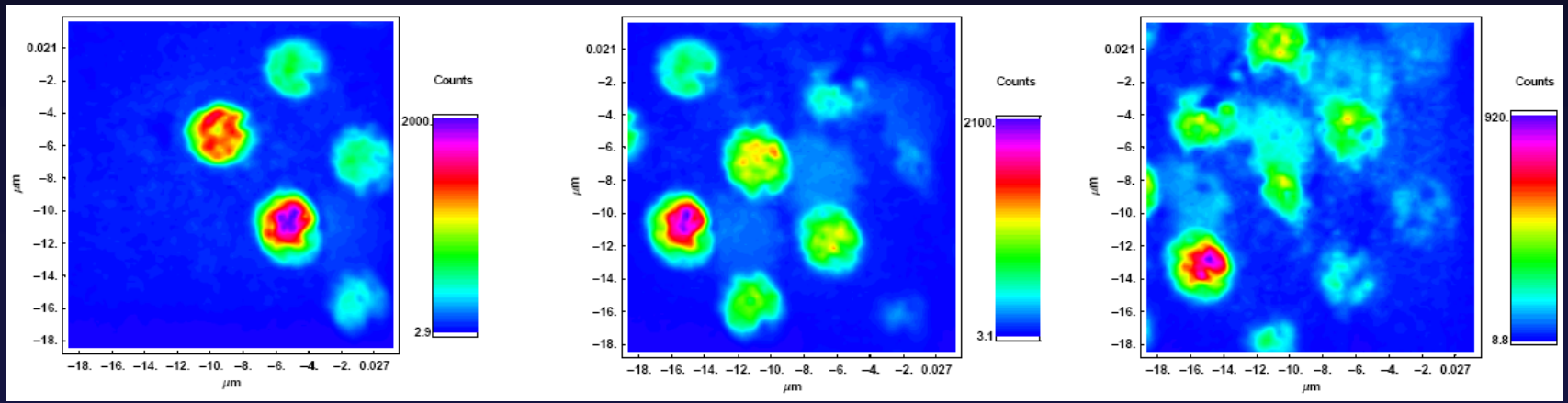

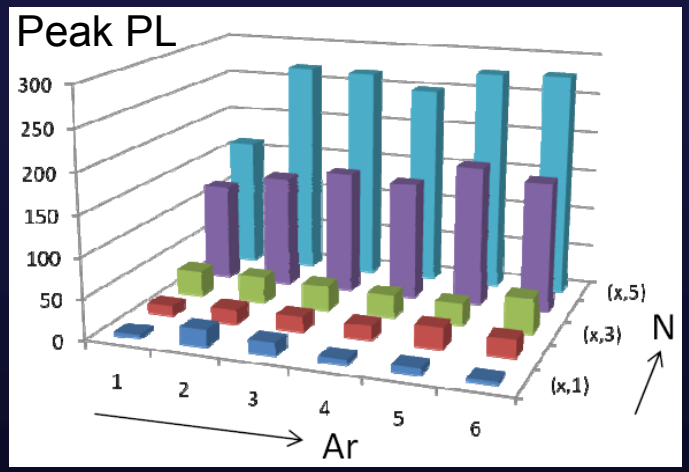

Greg Fuchs, David Toyli (UCSB)

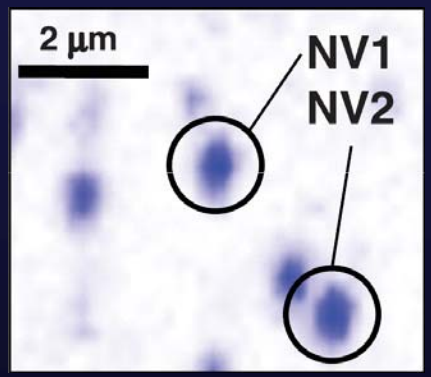

Fuchs et al., PRL 101, 117601 (2008)

Formation of NV- arrays by implantation of ^{15}N-ions with scanning probe alignment

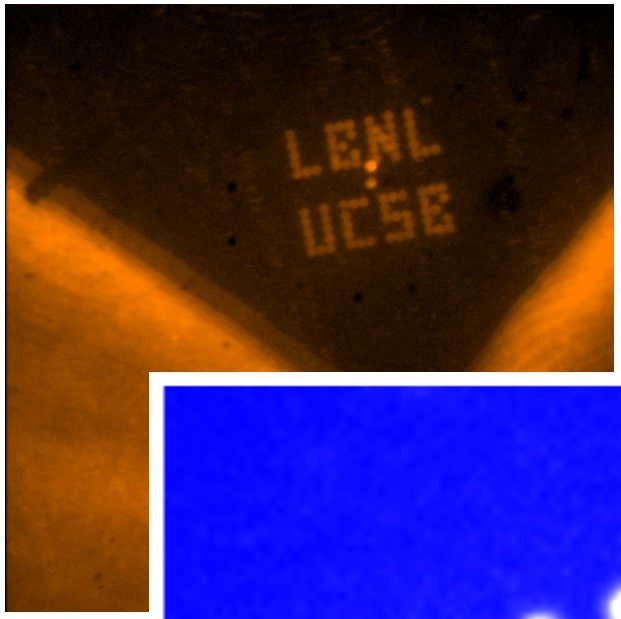

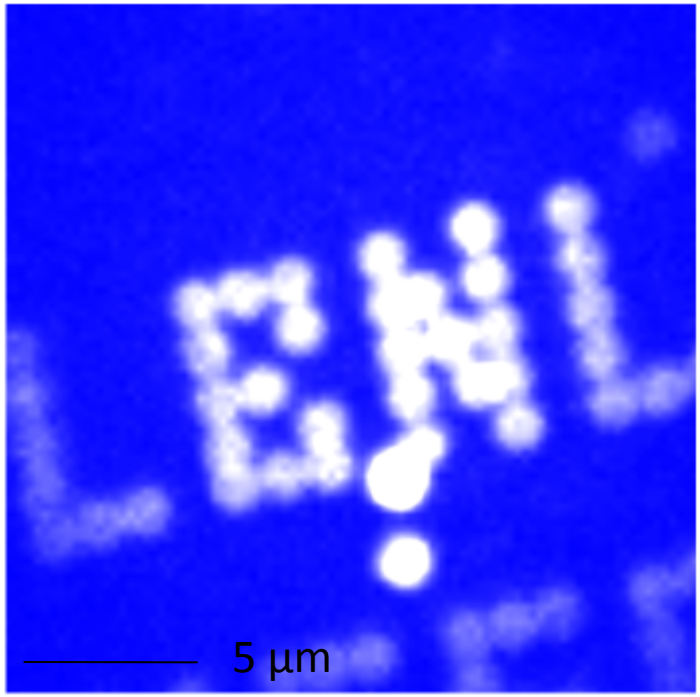

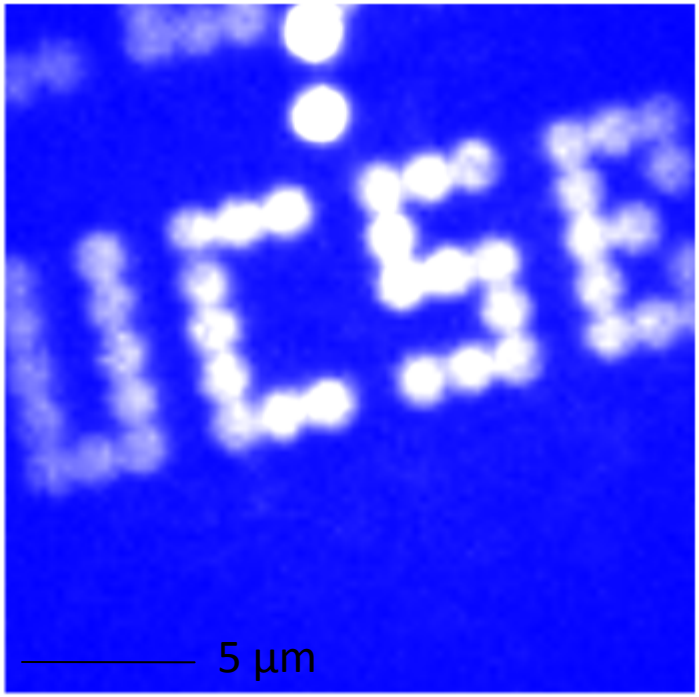

- photoluminescence images of NV^- centers after implantation of ^{15}N ions (high dose, 10^{12} $cm^{-2)}$
- dot diameter 1.2 microns, annealed at 850 C for 15 min. (bottom images courtesy of Greg Fuchs, UCSB)

Ion placement accuracy

STEM scan

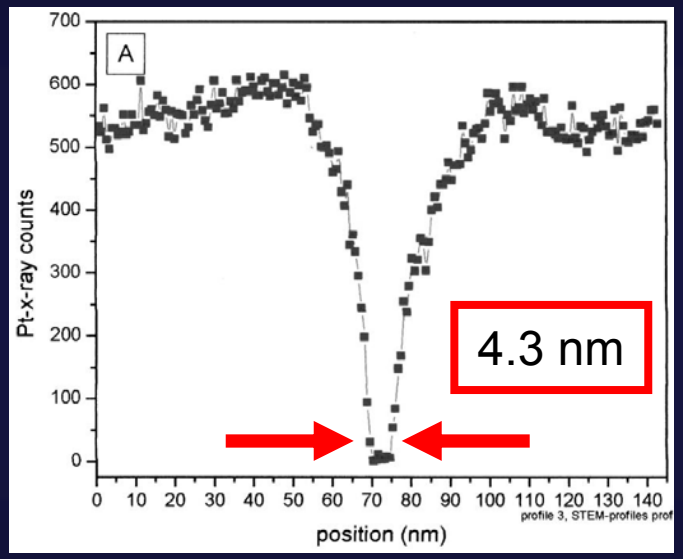

Schenkel et al., J. Vac. Sci. Technol. B, 21 (6), 2720 (2003)

80nm hole

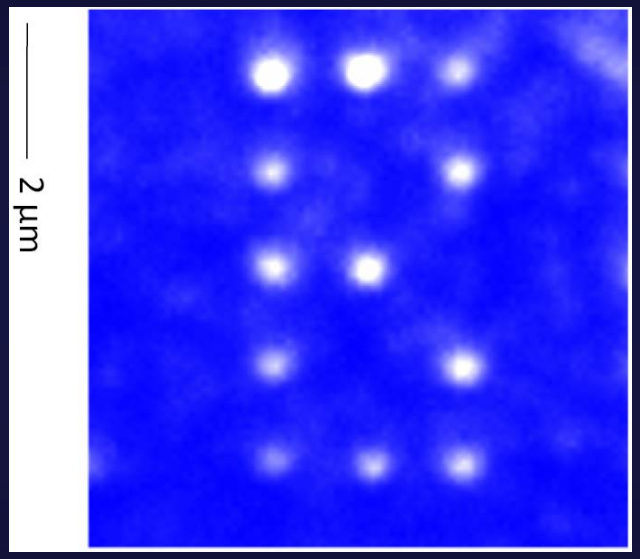

5-10 NV centers/spot
(unpublished)

Greg Fuchs et al. (UCSB)

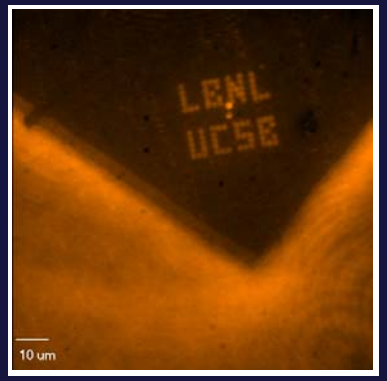

Optimization of NV-formation efficiency by defect engineering –
Argon co-implantation to find the local vacancy density optimal for NV- formation

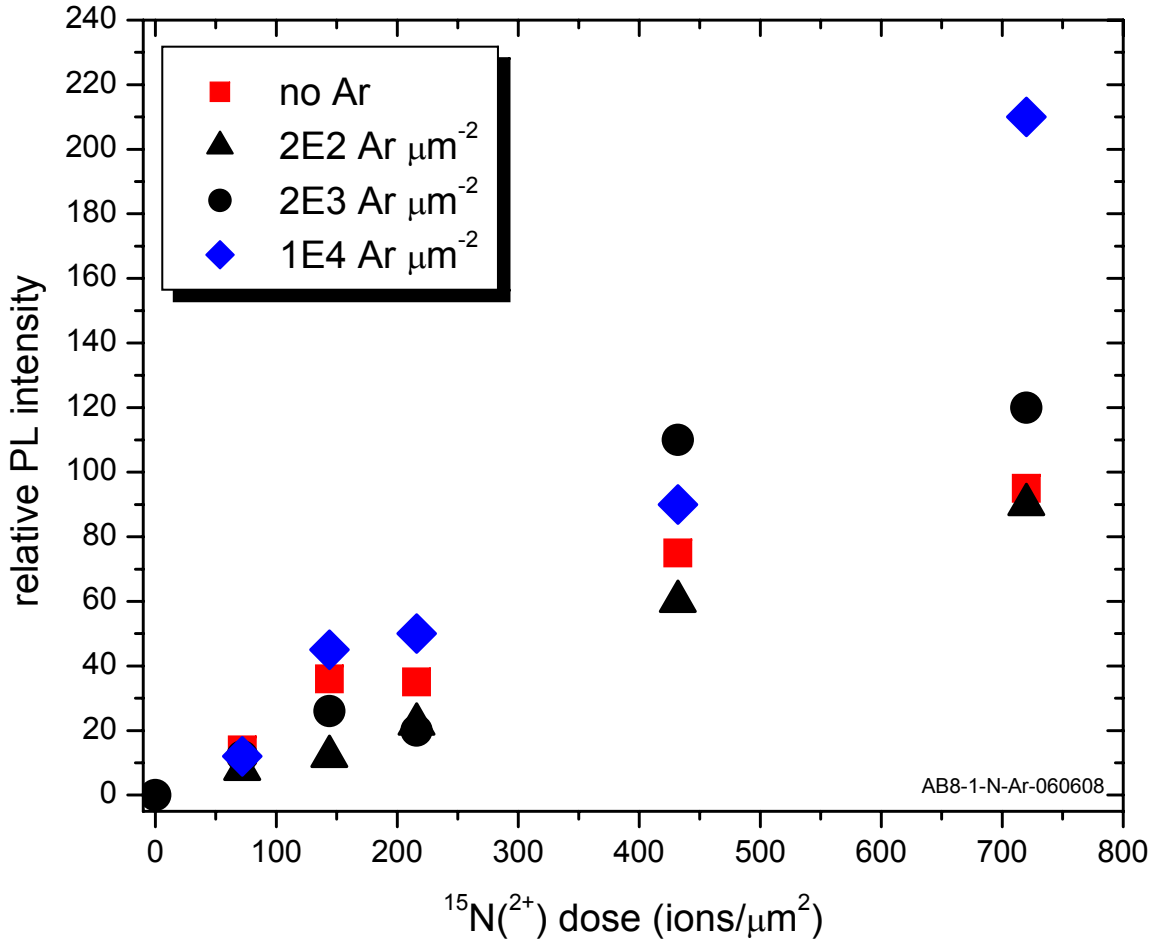

• implantation of 15-N (14 keV) together with increasing doses of Argon (28 keV)
• preliminary results indicate increased NV- formation probability with increasing Ar dose (after annealing at 800 C for 10 min.)

Excited-State Spectroscopy Using Single Spin Manipulation in Diamond

G. D. Fuchs,[1] V. V. Dobrovitski,[2] R. Hanson,[3] A. Batra,[4] C. D. Weis,[4] T. Schenkel,[4] and D. D. Awschalom[1]

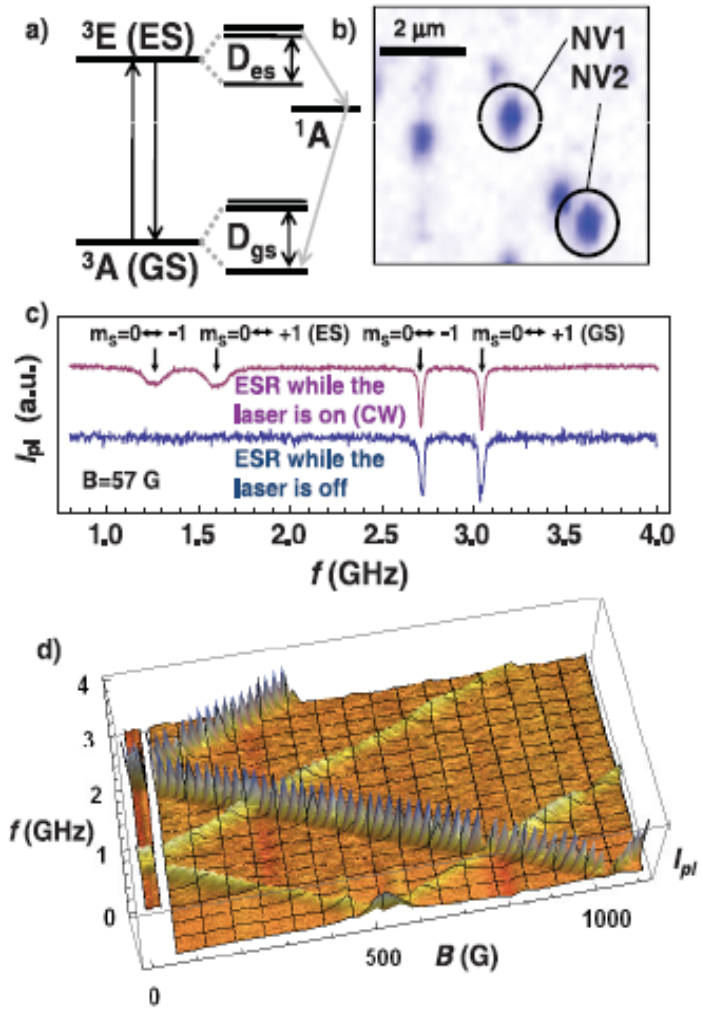

(a) Energy diagram of electronic and spin levels for a N-V center. Both the ground state (3A) and the excited state (3E) are spin triplets, with a zero-field splitting (D_{gs}, D_{es}) between the m_S=0 and the m_S=+/-1 levels. Black arrows show the largely spin-conserving optical transitions. There is also nonradiative relaxation through 1A that is not spin conserving (gray arrows indicate the dominate pathway). (b) Spatial photo-luminescence map with NV1 and NV2 indicated. We verified that each spot corresponds to a single N-V center using photon correlation measurements (not shown). (c) The top trace shows optically detected spin resonance at B=57 G where B_{rf} , laser illumination, and photon counters are all on continuously. The bottom trace is a measurement where Brf is applied while the laser is off so that the spin is manipulated only in the ground state. (d) Surface plot of cw spin resonance as a function of magnetic field. The viewpoint is below the data so that dips in Ipl appear as peaks. The sharp features are the GS spin resonances while the broad features are resonant transitions in the ES.

Spin Qubits in Diamond vs. Silicon

- coherence times ~ 1 ms for both
  - diamond N, NV: at 300 K
  - silicon donor: at 5 K
  - Si based quantum dot: unknown
- single spin control
  - demonstrated for single NV-centers
  - still rudimentary in silicon
- multi-qubit control
  - demonstrated for NV plus two ^{13}C nuclear spins (Wrachtrup group '08)
  - not shown in silicon
- high quality material available for both
  - any wafer size for Si
  - few mm^2 pieces for diamond

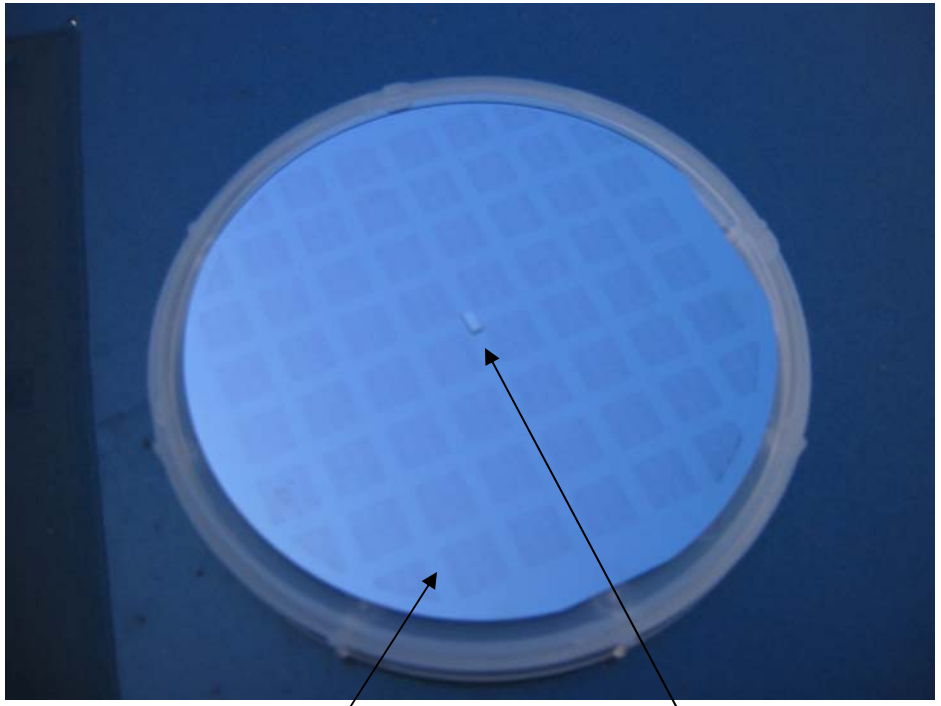

Acknowledgments

- **PostDocs**
  - Arun Persaud
  - Mohan Sarovar
- **Graduate students**
  - Christoph Weis (Technische Universität Ilmenau)
  - Cheuk Chi Lo (UC Berkeley)
  - Kevin Young (UC Berkeley)
  - Jianhua He (Princeton)
  - Shyam Shankar (Princeton)
- **Undergraduate students**
  - Andreas Schuh
  - Arunabh Batra
  - Dylan Gorman
- **Si-QC Team members**
  - Jeff Bokor, UC Berkeley & Molecular Foundry
  - Steven Lyon, Princeton University
  - Alexei Tyryshkin, Princeton University
  - Birgitta Whaley, UC Berkeley
- Diamond studies in collaboration with group of David Awschalom, UCSB
- **Special thanks to**
  - Staff of the UC Berkeley Microlab
  - Staff of the National Center for Electron Microscopy and ALS at LBNL
  - Staff of The Molecular Foundry at LBNL

This work is supported by LPS-NSA, NSF, and DOE